

UNCLASSIFIED

AD NUMBER

AD482287

LIMITATION CHANGES

TO:

Approved for public release; distribution is unlimited.

FROM:

Distribution authorized to U.S. Gov't. agencies and their contractors;
Administrative/Operational Use; JAN 1963. Other requests shall be referred to Naval Postgraduate School, Monterrey, CA.

AUTHORITY

NPS ltr 23 Sep 1971

THIS PAGE IS UNCLASSIFIED

066211

48228

copy

UNITED STATES
NAVAL POSTGRADUATE SCHOOL



THESIS

EXPERIMENTAL STUDY OF STRESSES
IN WELDED JOINTS

by
Casanave H. Young, Jr.

This document is subject to special export controls and each transmittal to foreign government or foreign nationals may be made only with prior approval of the U.S. Naval Postgraduate School.

Distribution Change Order refer to Change Authority Field



Private STINET

[Home](#) | [Collections](#)

[View Saved Searches](#) | [View Shopping Cart](#) | [View Orders](#)

Add to Shopping Cart

Other items on page 1 of your [search results](#): 1

[View XML](#)

Citation Format: Full Citation (1F)

Accession Number:

AD0482287

Citation Status:

Active

Citation Classification:

Unclassified

Fields and Groups:

130500 - Couplers, Fasteners, and Joints

Corporate Author:

NAVAL POSTGRADUATE SCHOOL MONTEREY CA

Unclassified Title:

(U) EXPERIMENTAL STUDY OF STRESSES IN WELDED JOINTS.

Title Classification:

Unclassified

Descriptive Note:

Master's thesis,

Personal Author(s):

Young, Casanave H , Jr

Report Date:

Jan 1963

Media Count:

75 Page(s)

Cost:

\$9.60

Report Classification:

Unclassified

Descriptors:

(U) *WELDS, *JOINTS, HYSTERESIS, MOMENT OF INERTIA, STRESSES, STRAIN GAGES, TEST EQUIPMENT, STEEL, EXPERIMENTAL DATA, TEMPERATURE, LOADS(FORCES), MODEL TESTS, INSTRUMENTATION, SHEAR STRESSES, TABLES(DATA), GRAPHICS

Identifier Classification:

Unclassified

Abstract:

(U) Design of welded joints is normally accomplished by the use of formulas which predict the stresses in the throat area of the welds. By means of metal foil strain gages the stresses were determined in three models of fillet welds; one subjected to a transverse load, one to a longitudinal load, and one to an eccentric load. Agreement was good for the transversely loaded fillet weld, and fair for the longitudinally and eccentrically loaded fillet welds. A modification of one of the assumptions made in the design of one type of eccentrically loaded fillet weld is suggested because it provides closer agreement between experimental and calculated stresses. (Author)

Abstract Classification:

Unclassified

Annotation:

Distribution Change Order refer to Change Authority Field

Experimental study of stresses in welded joints.

Distribution Limitation(s):

01 - APPROVED FOR PUBLIC RELEASE

Source Code:

251450

Document Location:

DTIC AND NTIS

Change Authority:

ST-A USNPS LTR, 23 SEP 71



[Privacy & Security Notice](#) | [Web Accessibility](#)

private-stinet@dtic.mil



EXPERIMENTAL STUDY OF STRESSES

IN WELDED JOINTS

Casanave H. Young, Jr.

EXPERIMENTAL STUDY OF STRESSES
IN WELDED JOINTS

by

Casanova H. Young, Jr.

Lieutenant Commander, United States Navy

Submitted in partial fulfillment of
the requirements for the degree of

MASTER OF SCIENCE
IN
MECHANICAL ENGINEERING

United States Naval Postgraduate School
Monterey, California

1963

EXPERIMENTAL STUDY OF STRESSES

IN WELDED JOINTS

by

Casanave H. Young, Jr.

This work is accepted as fulfilling
the thesis requirements for the degree of

MASTER OF SCIENCE

IN

MECHANICAL ENGINEERING

from the

United States Naval Postgraduate School

W. M. James
Faculty Adviser

R. E. Newton
Chairman
Department of Mechanical Engineering

Approved:

A. E. Jewell
Academic Dean

ABSTRACT

Design of welded joints is normally accomplished by the use of formulas which predict the stresses in the throat area of the welds. By means of metal foil strain gages the stresses were determined in three models of fillet welds; one subjected to a transverse load, one to a longitudinal load, and one to an eccentric load. Agreement was good for the transversely loaded fillet weld, and fair for the longitudinally and eccentrically loaded fillet welds. A modification of one of the assumptions made in the design of one type of eccentrically loaded fillet weld is suggested because it provides closer agreement between experimental and calculated stresses.

The writer wishes to express his appreciation for the assistance, encouragement, and especially the patience provided by Professor Virgil M. Fairless of the U. S. Naval Postgraduate School, in this investigation.

TABLE OF CONTENTS

Section	Title	Page
1.	Introduction	1
2.	Design of Models	3
3.	Testing Procedure	5
4.	Results and Discussion	9
5.	Conclusions	20
6.	Bibliography	21

APPENDICES

A	Sample Calculations	22
B	Analysis of Design Method of Eccentrically Loaded Weld Model by Superposition	30

End

LIST OF ILLUSTRATIONS

Figure		Page
1.	Design Convention for One Type of Eccentrically Loaded Weld	52
2.	Photograph of Longitudinally Loaded Weld Model	53
3.	Sketch of Longitudinally Loaded Weld Model	54
4.	Photograph of Transversely Loaded Weld Model	55
5.	Sketch of Transversely Loaded Weld Model	56
6.	Photograph of Eccentrically Loaded Weld Model	57
7.	Sketch of Eccentrically Loaded Weld Model	58
8.	Diagram of Strain-Gage Placement	59
9.	Typical Load-Versus-Strain Plot - Preliminary Runs	60
10.	Load-Versus-Strain Plot Showing Hysteresis Loop Cycles	61
11.	Typical Load-Versus-Strain Plot - Final Runs	62
12.	Photograph of Eccentrically Loaded Model and Holding Assembly on Testing Machine	63
13.	Photograph of Eccentrically Loaded Model and Holding Assembly on Testing Machine (Side view)	64
14.	Results of Tests of Longitudinally Loaded Weld	65
15.	Plot of Load Versus Strain for Longitudinally Loaded Fillet Weld (From Smith /6/)	66
16.	Results of Test of Transversely Loaded Weld	67
17.	Results of Test of Eccentrically Loaded Fillet Weld for Load Eccentricity of 6.5 Inches	68
18.	Results of Test of Eccentrically Loaded Fillet Weld for Load Eccentricity of 8.5 Inches	69
19.	Results of Test of Eccentrically Loaded Fillet Weld for Load Eccentricity of 10.5 Inches	70
20.	σ_x Stress Distribution for Eccentrically Loaded Fillet Weld	71

List of Illustrations (Continued)

Figure		Page
21.	σ_x Stress Distribution for Eccentrically Loaded Fillet Weld	72
22.	τ_{xy} Stress Distribution for Eccentrically Loaded Fillet Weld	73
23.	Plot of Load Eccentricity Versus Shift of Turning Center	74
24.	Computer Programs for Data Reduction and Design	75

SYMBOLS AND ABBREVIATIONS

Symbols

b	- weld size
c	- a constant
d	- distance between welds
E	- Young's Modulus
e	- eccentricity
F	- Force, Load
G	- centroid
J	- moment of inertia, polar
L	- weld length
t	- throat dimension of weld
μ	- Poisson's ratio
ρ	- variable distance
σ	- normal stress
σ_1	- maximum normal stress
σ_2	- minimum normal stress
τ	- shear stress

Abbreviations

ave.	- average
calc.	- calculated
exp.	- experimental
kip	- kilo pounds, 1000 pounds
ksi	- kips per square inch
lbs.	- pounds
max.	- maximum

1. Introduction.

For many years the design of welded joints has been based on formulas that approximate the average state of stress in the weld. For most joints there is an abundance of experimental evidence to support the safety of these approximations. Most of this evidence is in the form of results of tests to destruction of a representative sample of models of different joints. In the late 1920's and early 1930's, the literature shows a lively interest in such tests as well as various analyses of the theory of stresses in welds. Growing out of these tests and analyses was a set of design approximations. Jennings /1/ seems to have presented the most complete set of analyses which is still widely used.

For eccentrically loaded fillet welds of the type shown in Fig. 1, page 52, a search of the literature revealed no direct experimental verification of the safety of the design convention given in "Procedure Handbook of Arc Welding Design and Practice", /2/ and Faires /3/. Nor could there be found any experimental justification for the assumptions made.

The object of this project is to study the correlation between the computed stresses and those actually measured in order to investigate the validity of the design procedures for:

- A. A longitudinally loaded fillet weld, Figs. 2 and 3, page 53 and 54
- B. A transversely loaded fillet weld, Figs. 3 and 4, page 55 and 56
- C. An eccentrically loaded fillet weld, Figs. 5 and 6, page 57 and 58

For the longitudinal and transverse weld models, the investigation was by means of a direct comparison of calculated and experimental stresses. For the eccentrically loaded model two methods were attempted. First, a direct comparison of calculated and experimental stresses. Second, it was postulated that the resultant shear stress could be obtained by superposing shear stresses induced by three distinct resisting mechanisms. The shear stress distribution for each was determined from the results of the longitudinal and transverse

weld tests. Then the stresses were computed, superposed, and then compared to the experimental stresses found in the eccentrically loaded weld model. This procedure is given in Appendix B.

Strains were measured by means of metal-foil rosette strain gages placed on the machined weld surfaces.

The project was conducted by the author in the Materials Testing Laboratory of the U. S. Naval Postgraduate School, Monterey, California under the supervision of Professor Virgil M. Faires, during the period January to May 1963.

2. Design of Models.

The size of all models was dependent upon the size of available rosette strain gages. Since miniature gages of one quarter inch in diameter were available from Baldwin-Lima-Hamilton, a 0.350-inch fillet weld was decided upon. This size provides a hypotenuse on the fillets of about one-half inch and thus allows a reasonable clearance for the gages and some space for the installation of leads. Although this clearance seemed adequate, it proved none too much. Balanced against the desirability of adequate clearance is the effort to keep weld sizes down to a minimum so as to reduce model size. Also smaller welds with fewer passes of welding tend to be more uniform.

A Riehle Testing Machine Type PSC - 120 of 120,000-lbs. capacity was used to load models A and B. Thus requirements for the size of the tongues were such that they would fit into the grips of the machine. The lengths of the welds were such that the machine could load the models to the elastic limit of the welds. Double straps were used to minimize a bending on the weld when the model was loaded in tension. In addition was the desire to conform, in general, with the specifications of the transverse fillet weld test specimens as given in "The Welding Handbook" of the American Welding Society. /4/

The models were made of mild steel. This was used since it was on hand and because it is weldable without unusual difficulties. For strength estimations a tensile design stress of 50,000 psi and a design stress in shear of 30,000 psi were used. Electrodes of E-6013 were used for welding, which was done by the best qualified welder at the U. S. Naval Postgraduate School.

Both models A and B when loaded to the full 120,000-lbs. capacity of the machine have a minimum factor of safety based on the tensile yield point of about 1.5 except in the welds themselves.

For the eccentrically-loaded model it was necessary to design a holder assembly to support the model during loading. Photograph of model and holding assembly is shown in Fig. 6, page 57. Sketches of the model are shown in Fig. 7, page 58.

The entire assembly for model C is designed to be placed on the table of a Riehle, Model PS-300, testing machine. Forward and backward movement allows the eccentricity of the load to be varied over a considerable range. Transverse alignment is provided by keying the holding assembly to slots in the weighing table. Two symmetrical plates were used to apply the load to the welds so as to reduce the tendency of the plates to warp or twist when loaded.

The materials were the same as for models A and B. The strength of holder assembly and model allows the welds to be loaded almost to the limit of the elastic region.

3. Testing Procedures

Longitudinal and Transverse Weld Models

For both the longitudinal weld model and the transverse weld model, the method of testing was the same and the description will apply to both.

The models were placed in the testing machine and aligned so as to give virtually a tensile load. This requirement presented some difficulty. Although care was taken to eliminate bending loads by careful design and construction of models some bending undoubtedly existed. The models were symmetrical about the center line, so as to balance the load between the left and right. On the longitudinal model, one rosette was placed on the weld opposite to the weld under study in order to determine the distribution of load between left and right. In addition, two A-5 type strain gages were placed on the plate of this model for the same purpose. For the transverse weld, the strains in the end rosettes were compared. It was assumed that equal strain readings from gages placed symmetrically about the center line was an indication of the absence of bending. Prior to making final runs, several preliminary runs were made to adjust the strain indications to as nearly the same values as possible. Adjustments were made by shims and by re-seating the chucks into the tongues of the models.

Four rosettes were mounted along the length of each weld under study, as shown in Fig. 8, page 59. The elements of the rosettes were connected into a Baldwin-Lima-Hamilton Switching and Balancing Unit.

Temperature compensation was provided by an element of a rosette mounted on a machined weld bead on a plate of the same material as the model. Strain indications were measured by a Baldwin-Lima-Hamilton SR-4 Type N Strain Indicator.

Initial runs indicated little consistency of data when the start was from zero load. This is believed to have been due to failure of the chucks to seat firmly and completely under light load. Measuring from an arbitrary load of

several runs where the chucks were more firmly seated seemed to eliminate this difficulty.

Load was increased in increments of several kips and the strain at each element was read. Strain was measured during both loading and unloading on the first runs, which were well within the elastic limit of the welds. A plot of load versus strain was prepared for each element of the rosettes. A typical plot is shown in Fig. 9, page 60. It is noted that the load-strain curve is not linear on either loading or unloading. Further, the appearance is suggestive of a hysteresis loop, with the unloading curve returning to the arbitrary reference point. When the arbitrary reference point was altered the first cycle usually showed a small amount of set. Subsequent cycles showed a tendency for the loops to close. This effect is shown in Fig. 10, page 61. The cause of the loop is not known and was the subject of considerable investigation. It is discussed at the end of this section.

For the final runs of the transverse and longitudinal models, it was intended to load to the limit of the elastic range. This was expected to correspond to a load of about 120 kips for the longitudinal model and about 60 kips for the transverse model. However, for loads in excess of about 40 kips there was considerable difficulty in obtaining data because of a tendency for the models to slip in the chucks. Slipping was evidenced by an audible sound, an instantaneous drop of two or three kips on the load indicator while the chucks reseated, and a discontinuity of the data. Many runs were made with each model before runs high enough were obtained. The final run for the transverse model was to a load of 66.8 kips, where the chucks slipped. The longitudinal model was finally loaded to 97.4 kips where the chucks slipped. For both models, the final strain readings before slipping showed discontinuities. This may be due either to a gradual tearing of the chuck teeth thru the tongues of the model before letting go, or yielding of the welds. Because of the uncertainty of this final reading it was not considered. In the case of

the transverse model, there was some evidence of local yielding at the left end. Because of the discontinuity of data after the chucks slipped, data were not taken during unloading in the final runs.

Plots of load versus strain for the final runs for typical gage elements of both models are shown in Fig. 11, page 62. It is noted that for the longitudinal welds the tendency to loop is less than it was for earlier runs to lesser loads. The curves for the loading of the transverse model are now quite linear.

Eccentrically Loaded Model

The eccentrically loaded model and holder on the weighing table of the Riehle PS-300 Universal Testing Machine is shown in Figs. 12 and 13, pages 63 and 64. Load is applied by the lower head.

Several preliminary runs were made in order to adjust the distribution of the load equally between the welds on either side of the central plate. Four rosettes were mounted along the length of the weld under study. Again one rosette was mounted on the opposite weld to assist in minimizing twisting. By adding shims it was possible to adjust the strain readings on the elements measuring strain along the longitudinal axes of the welds to within about 5% of each other.

Three working runs were made. The eccentricity of the load about the centroid of the weld area was varied. Runs were made for eccentricities of six and one-half inches, eight and one-half inches, and ten and one-half inches. Loads were such as to induce stress levels of about the same values for each of the eccentricities.

Instrumentation was the same as for the transverse and longitudinal runs. Readings were taken during loading and unloading for all runs, which revealed a looping in the curves of load versus strain.

Discussion of Hysteresis Loops

The looping is not clearly understood. Investigation and check of instrumentation eliminated the possibility of this cause. Other causes considered

were:

a) That the area of the loops represented a measure of the energy lost by the frictional work caused by the relative motion between plate and strap. This was checked by deliberately increasing the normal force between plate and strap by means of large C-clamps. Experiment showed that the total resisting force was markedly increased, since the slope of the load versus strain diagrams increased. Also the area of the loops increased. This shows that the increase in frictional force resulted in an increase in the area of the hysteresis loop, and thus frictional energy lost is probably responsible for the increase in loop area. It may be responsible for the original loops. If the cause of the loops was wholly due to frictional energy, it would be expected that a line symmetrically dividing the loop would represent the true load versus strain plot. It was found that such lines drawn on loops to different maximum loads produced slightly different slopes. Therefore it is concluded that friction may contribute to the loops, but is probably not the sole cause.

b) The loops have the appearance and the properties of those caused by elastic hysteresis as discussed by Timoshenko /5/. This is considered a possible cause.

c) It was observed that the looping effect was greater for preliminary runs of the transverse and longitudinal models than for the final runs. This may be due to plastic strain and work hardening of the weld metal.

4. Results and Discussion.

A. Longitudinal Model

Results

The results of tests of the longitudinal model are shown in Fig. 14, page 65. The principal stresses σ_1 and σ_2 and the maximum shear stress τ_{max} are plotted as they vary along the length of the weld. The principal directions are indicated along the weld length. Both are for a load of 21 kips per weld.

COMPARISON OF STRESSES FOR LOAD OF 21 KIPS PER WELD

$\tau_{cal. (eq. 1)}$	$\tau_{max. exp.}$	$\tau_{ave. exp.}^*$
21.2 ksi	19.3 ksi	10.0 ksi

Discussion

The design formula for this type of joint as given by Yaires /3/, and others, is:

$$(1) \quad \tau = \frac{0.707F}{bL}$$

where F is the load transmitted thru one strap,

b is the weld size (leg)

L is the weld length.

Discussion

It is well known that the stress in fillet welds is not uniform. Smith /6/ performed a series of experiments at the University of Pittsburgh in 1929 and 1930 of double-straped plates. Each strap was connected by two longitudinal fillet welds to the plate. The displacement of the straps relative to the plate was measured mechanically at several sections. The results were presented in a series of plots showing longitudinal displacement as a function of length along the weld. These tests showed the strain to be

* Values reported as average were obtained by determining the area under the curve and dividing by the base.

greatest at one end, and to tend toward a minimum at the center. The general shape of the curves being a function of the ratio of the cross-sectional area of the plate to the sum of the cross-sectional areas of the two straps. These results are shown in Fig. 15, page 66. It is noted that as the ratio of the areas increases, the point of minimum strain tends to shift from the joint end toward the center, the maximum strain being at the free end for ratios less than unity. For ratios of the areas of unity, the curves are roughly symmetric. No data are shown by Smith /6/ for ratios greater than unity. In this experiment, the ratio of plate area to strap area was 1.75. Figure 14, page 65 shows that the maximum strain is at the joint end. It is also evident that at the free end the strain does not increase above the value near the center as might be expected from an extrapolation of Smith's results.

Goodier and Hsu /7/ report an experiment in which strain-gage measurements were made on a monolithic model of a bar and a plate. The gages were mounted on the center line of the bar. The results show that for a four-inch bar at sections near the joint side, the longitudinal strain decreases rapidly within the first inch, then more gradually until the end. The ratio of cross-sectional area of plate to cross-sectional area of the strap is not given but, from the illustration given, it is obviously considerably greater than unity. This seems to provide some confirmation for the results as shown in Fig. 14, page 65, with regard to the stress at the free end.

The comparison of T_{max} calculated by equation (1) and T_{max} experimental seems quite close. However, the strains were measured on the free boundary of the welds. The average strain through the throat section is undoubtedly greater. Photoelastic studies by Solakian /8/ show that for transverse fillet welds the ratio of average stress to surface stress is about three to two. Shreiner /9/ tested fillet welds in bending and shear and concluded that the ratio of average stress to surface stress was about three to two. If the

experimental value of τ_{max} is increased by the ratio of average stress across the throat to surface stress (use 1.5 in the absence of better information), the value obtained is 28.9 ksi compared to the calculated value of 21.2 ksi. Using the factor of 1.5, the average shear stress along the weld is 15 ksi compared to the calculated value of 21.2 ksi. The ratio of stress at the end of the weld (28.9 ksi) to the average stress (15 ksi) is 1.93. This value is less than the stress concentration factor of 2.7 for the toe of a longitudinal fillet weld.

The orientation of the principal axes in Fig. 14, page 65 shows that the direction of maximum shear stress very nearly runs along the longitudinal axis of the weld. This confirms the accepted concept that the longitudinal weld is best designed on the basis of shear stresses.

B. Transverse Model

Results

The results of the tests of the transverse model are shown in Fig. 16, page 67. The principal stresses σ_1 , σ_2 , and the maximum shear stress τ_{max} are plotted as they vary along the length of the weld. The principal directions are indicated along the weld length. Both are shown for a load of 30 kips per weld. In the first comparison below, the stress calculated is

COMPARISON OF STRESSES FOR LOAD OF 30 KIPS PER WELD

<u>$\tau_{calc. (eq. 3)}$</u>	<u>$\tau_{max. exp.}$</u>	<u>$\tau_{ave. exp.}$</u>
30.3 ksi	20.6 ksi	19.0 ksi
<u>$\sigma_1, calc.$</u>	<u>$\sigma_1, max. exp.$</u>	<u>$\sigma_1, ave. exp.$</u>
30.3 ksi	49.0 ksi	43.0 ksi

taken as a shear stress. In the second comparison the calculated stress is considered as a normal stress.

The direction of the principal axes indicate a lack of symmetry of normal stresses. Symmetry considerations would require the σ_1 axis at station three to be inclined to the left. This stress distribution may be due to any one or a combination of the following:

a) One or more faulty elements in the rosette at station three.

b) Error in gage placement. This gage was erroneously placed with its center about 1/16 inch above the weld-face center line. In addition it was not placed symmetrical to the gage at station two. See Fig. 8, page 59.

c) Uneven load distribution.

With regard to the stresses in joints with transverse loading, Jennings /1/ states, "In the generally accepted method of computing stresses in transverse fillet welds it is assumed that the stress at the throat section is principally a normal tensile stress." This stress is calculated from;

$$(2) \quad \sigma = \frac{1.414F}{Lb}$$

where F is the load transmitted thru one strap (two welds), b is the weld size, and L is the weld length. The equation is also found in The American Welding Society Handbook /4/.

The ratio of $\tau_{\text{calc.}}$ to $\tau_{\text{max.exp.}}$ for the transverse model is about three to two. The ratio of σ_1 calculated as recommended by Jennings and The American Welding Society Handbook to $\sigma_{1 \text{ max.exp.}}$ is about three to five. Thus, if one designs on the basis of normal stress, a larger design factor is indicated to provide the same degree of safety.

Other authorities including Timoshenko /5/ and Fairies /3/ note that the design of transverse fillet welds is usually based on an assumed shear stress across the throat section; that is,

$$(3) \quad \tau = \frac{1.414F}{Lb}$$

Gillespie, Hughes, Jackson, and Fox /11/ report that "Normal welds, other things being equal, are stronger than parallel welds," a generally recognized relationship. Their curves show that the strength of transverse fillet welds

to about 130 per cent that of longitudinal fillet welds.

The results of the test of the transverse model show that for four inches of weld, a load of one-kip produces a maximum shearing stress of 0.586 ksi. The results for the longitudinal model show that for four inches of weld a one-kip load produces a maximum shearing stress of 0.919 ksi. Since a given load produces a smaller maximum stress in the transverse weld than the longitudinal weld, the transverse weld can safely withstand a larger load. For this case the ratio of the shear stresses shows that the strength of the transverse weld is about 134 per cent ($\frac{.919}{.586} \times 100$) that of the longitudinal weld. This is in good agreement with other similar experimental values.

If one were to design on the basis of shear stress, the results of this experiment show that the calculated value will be greater than the actual stress that will exist in the weld. If the ratio of three to two discussed on page 10, is applied, the actual average stress is almost exactly that calculated. On the other hand, if normal stresses are considered to be the basis for design, the results indicate that the actual normal stress (σ_1 times 7/2) is 2/3 per cent of the calculated stress. The conclusion is that design based on the average shear stress rather than the normal stress is the better.

C. Eccentrically Loaded Model

When two welds are used to prevent a turning, as in the eccentrically loaded model, the conventional method of design is first to assume that the center of rotation is at the centroid G of the welds, approximated with the throat area, considered mathematically as a line. (See Fig. 1, page 52). Next it is assumed that the stress produced by the moment T_e , at any point on the length of the weld is directly proportional to the point's distance from the centroid G. As shown by Timoshenko (3), the equation for the stress f at the point is, $f = \frac{T_e y}{I}$.

$$(2) \quad \tau_1 = \frac{F e}{J_c}$$

where J_c is the moment of inertia of the throat area of the welds with respect to the centroid. This stress τ_1 is assumed to be in a direction normal to the radius vector from the centroid.

Next the load F is assumed to cause an average downward shear stress given by,

$$(3) \quad \tau_2 = \frac{F}{2tL}$$

where t is the throat dimension of the weld and L is the length of the weld.

The vector sum of τ_1 and τ_2 is assumed to be the maximum shear stress,

$$\tau_{\max}$$

Results

The results of the tests of the eccentrically loaded model are shown in Figs. 17, 18 and 19, pages 68, 69 and 70. These illustrations show $\tau_{\max \text{ calc}}$ and $\tau_{\max \text{ exp}}$ plotted against the distance along the weld. The orientation of the principal axes at each of the four rosette stations is also shown.

Table 14, page 51 shows a tabulated comparison of experimental and calculated values of maximum and average shear stress for each of the values of load eccentricity. It also shows a comparison of the ratios of $\tau_{\max \text{ calc}}$ to $1.5 \tau_{\max \text{ exp}}$ for each value of load eccentricity.

Discussion

The objective of the tests with the eccentrically loaded model was to obtain experimental stresses for comparison with computed values of stress. Hopefully the results would indicate a close correlation. Figures 17, 18, and 19, pages 68, 69 and 70, show a reasonably close correlation; especially in view of the nature of the assumptions used in the design approximations. Study of the figures and tables 11, 12, and 13, pages 48, 49 and 50 show

that as the eccentricity of load increases, the maximum stress on the experimental curve approaches, and in the most eccentric case, exceeds the calculated value of stress. Ideally, the computed and experimental curves should be such that the ratio of calculated stress to experimental stress is constant. While these curves approach the ideal in the left portion where the stresses are the lowest, they do not in the region of maximum stress. On the basis of the average stress, the calculated values appear safe.

If the experimental stresses are increased by a ratio of three to two (the approximate ratio of average stress across the throat section to surface stress, page 10), the experimental curves will fall closer to the calculated curves in the left portions. In the right portion they will exceed the calculated values, suggesting that welds with this type of loading are not as safe as the conventional design calculations indicate.

Several alternate methods of design were considered in an effort to determine a procedure that would result in better correlation with experimental data. Some of these methods provided stress values that agreed closely with the average experimental stress. Some agreed well with the actual stress distribution along the weld. Figures 20, 21 and 22, pages 71, 72 and 73, show the distribution of the normal stress along the weld σ_x , the normal stress perpendicular to the weld σ_y , the shear stress along the weld axis τ_{xy} . It is apparent that the pattern is complex. Therefore, it is unlikely that any relationship that might be found to describe the conditions would still be simple enough to be useful as a design tool.

Efforts were made to improve on the conventional design procedure for a specimen such as the model used. The method of attack was to consider the assumptions, to assess their validity; and to consider the effect of modifying them.

The assumptions were

- a) The center of turning is at the centroid.
- b) The stress, T_1 , due to the external moment P_e is directly proportional to the distance from centroid to point in question.
- c) The direction of T_1 is normal to the radius vector from the centroid.
- d) The component of downward shear stress, T_2 , induced by the load is uniform.
- e) T_{max} is the vector sum of T_1 and T_2 .

Experimental evidence shows that the stress in the end nearest to the load increases more rapidly than is predicted by calculation. Therefore, one or more assumptions are in error, at least to a degree. Consider the assumptions in sequence. The effects of possible change are:

a) If turning were considered about some point d' more remote from the load than O , then ρ would increase on the side near the load, and decrease on the opposite side. This would tend to produce the desired change in T_1 and T_{max} .

b) The stress T_1 could be considered to be greater than directly proportional to ρ . For example, $T_1 \propto \rho(x/L)^2$, where x is the distance from the left end of the weld and L is the length of the weld. This possibility was rejected as being too empirical as well as too complex.

c) T_1 could be considered other than normal to the radius vector, ρ . This possibility was rejected since this is the only logical direction for T_1 on the basis of the conventional design equation.

d) T_2 , the vertical shear stress induced by the load applied transversely to the welds could be considered non-uniform. This possibility was rejected since the tests of the transversely loaded weld showed such stress

to be nearly uniform.

The assumption that the vector sum of T_1 and T_2 was a reasonable approach to get T_{max} seemed acceptable.

It was decided to investigate the effect of moving the center of turning G along the longitudinal center line (See G' in Fig. 1, page 52). This assumption would have the effect of increasing ρ , and thus T_1 , the stress at the end near the load, while decreasing it to a lesser extent at the opposite end. Also the increase in the moment arm e , of the force F , would produce an increase in stress T_1 at all points of the weld. It was noted previously that as the eccentricity of load increases, the tendency for the calculated stress at load end of the weld to be proportionally low increases. For lack of more complete evidence, it was assumed that the amount of shift of the turning center varies directly with the eccentricity of the load with respect to the centroid.

A series of calculations was made to determine the location of the center of turning, such that the correlation of the calculated stresses and experimental stress would be as closely optimum as possible. Optimum correlation was considered to exist when:

1) $T_{max\ cal}$ equals 1.5 $T_{max\ exp}$ (the 1.5 adjusts surface stress to average stress across throat).

2) The shape of the curve of T_{max} versus distance along the weld was the same for experimental and calculated values.

The calculation procedure was as follows:

1) The location of G' , a point of turning was assumed; T_{max} was calculated for station one. It was compared with the experimental value. If it was not closely 1.5 times the experimental value, a new turning point was assumed and the calculation repeated until agreement was obtained. Then

T_{max} were computed for the remaining stations. The shape of the shear stress curve was compared with the experimental curve. If the shape was not the same, the stresses for all stations were calculated for other values of turning point location. The final recommendation is a compromise of the two conditions of optimum correlation.

2) The same procedure was followed for a second loading condition.

3) A plot of eccentricity of load (with respect to the centroid C) versus shift of center of rotation GC' was made. (See Fig. 23, page 74). The two points obtained by iteration were plotted. In addition a point was located for zero center shift. The best straight line was drawn through these three points. This line determined a predicted value of center of turning shift for the third case of eccentric loading.

4) Using the predicted value of turning point shift, the center of turning was determined for the third case of load eccentricity. Calculations for T_{max} were made for all stations. Considerable improvement in correlation was noted. Then a set of calculations were made for turning points to the left and right of the predicted value. Correlation, as before not ideal, was apparently best at the predicted value. The calculated values of T_{max} using the turning centers determined are shown on Fig. 17, 18, and 19, pages 68, 69 and 70. Tables 11, 12, and 13, pages 48, 49 and 50, show a comparison of the ratio of $T_{max cal}$ and $1.5 T_{max exp}$ for G and for various values of G' . In addition the tables show a comparison of the angle of orientation (θ) of the principal axis with the longitudinal axis of the weld.

It is seen that the selection of the curve that provides best correlation is difficult; the one finally being selected must represent a compromise between good agreement at the high end and good agreement throughout

the length of the curve.

The following facts seem to be indicated:

1) Better correlation between calculated stress and actual stress is obtained if it is assumed that the center of turning is located more remote from the load than the centroid.

2) The greater the eccentricity of load with respect to the centroid, the more the center of turning shifts.

In order to utilize this knowledge in the design of welded joints of this type, a relationship for the shift of turning center as a function of load eccentricity would be useful. Figure 23, page 74 indicates a shift of turning center of 0.117 inches for each inch of eccentricity (with respect to the centroid) of applied load. Considering the nature of the problem, it is concluded that a good approximation for welds of the proportions of the eccentrically loaded model would be: let the turning center be moved 10 per cent of the eccentricity e , (Fig. 1, page 52) further from the point of application of the load. If it is desired to be more conservative, a greater shift may be used.

5. Conclusions.

Based on the results of the tests of this project the following conclusions are drawn:^{*}

A. For longitudinally loaded fillet welds:

The maximum shear stress in the weld is approximately 136 per cent of the calculated value. The average shear stress along the length of the weld is approximately 71 per cent of the calculated value.

B. For transversely loaded fillet welds:

The maximum shear stress in the weld is less than 2 per cent greater than the calculated value. The average shear stress along the length of the weld is approximately 6 per cent less than the calculated value. Design of transverse welds on the basis of normal stresses is unsafe. Design on the basis of shear stresses is the best method.

C. For eccentrically loaded fillet welds:

The maximum calculated shear stress averages 65 per cent (Table 14, page 51) of the experimental value for the three cases of load eccentricity.

The average calculated shear stress along the length of the weld averages 109 per cent of the experimental value for the three cases of load eccentricity.

The design convention is improved by assuming that the center of turning of the welds is more remote from the load than the centroid. A suggested method of locating the center of turning is to assume that the point shifts away from the centroid ten per cent of the amount of the eccentricity of the applied load with respect to the centroid of the welds. For computing the applied moment and corresponding shear stress, the moment arm of the applied load is measured to the turning center thus located.

^{*} A factor of 1.5 representing the ratio of average stress across the throat section to the surface stress on the weld has been used in arriving at values stated.

BIBLIOGRAPHY

1. C. H. Jennings, Welding Design, ASME Transactions, Vol. 38, p. 497.
2. The Lincoln Electric Co., Procedure Handbook of Arc Welding Design and Practice.
3. V. M. Fairer, Design of Machine Elements, The Macmillan Co., 3rd Edition, New York, 1935.
4. American Welding Society, Welding Handbook, Section One, 4th Edition, 1937.
5. S. Timoshenko, Strength of Materials, Part II, D. Van Nostrand Co.
6. J. Hammond Smith, Stress Strain Characteristics of Welded Joints, Journal of the American Welding Society, Sept. 1929.
7. J. M. Goodier and C. S. Hsu, Transmission of Tension From a Bar to a Plate, Journal of Applied Mechanics, Vol. 21, No. 2, June 1954.
8. Arshag G. Solakian, Stresses in Transverse Fillet Welds by Photoelastic Methods, Journal of The American Welding Society, Vol. 13, No. 2, Feb. 1934.
9. Norman G. Schraier, The Behavior of Fillet Welds When Subjected to Bending Stresses, Journal of The American Welding Society, Vol. 14, No. 9, Sept. 1935.
10. S. Timoshenko and G. H. MacCullough, Elements of Strength of Materials, D. Van Nostrand, Co.
11. Peter Gillespie, C. A. Hughes, K. B. Jackson, J. H. Fox, Report on Pilot Tests Conducted for The Structural Steel Welding Committee of The American Bureau of Welding at The University of Toronto, 1927-28.

APPENDIX A, SAMPLE CALCULATIONS

Subject

1. Determination of calculated values of shear stress for the longitudinal, transverse, and eccentrically loaded model.
2. Reduction of data from measured strains to stress.

1. Determination of calculated values of stress for the longitudinal, transverse, and eccentrically loaded models

A. LONGITUDINAL MODEL

From data, Table 1 and Fig. 3.

F = 84 kips total; 42 kips per strap

b = 0.35 inches; L = 4 inches

From equation (1),

$$\gamma = \frac{0.707F}{bL} = \frac{0.707(42)}{(0.35)(4)} = 21.2 \text{ ksi.}$$

B. TRANSVERSE MODEL

From data, Table 2 and Fig. 5.

F = 60 kips total; 30 kips per strap

b = 0.35 inches; L = 4 inches

From equation (2),

$$\sigma = \frac{1.414F}{bL} = \frac{1.414(30)}{0.35(4)} = 30.3 \text{ ksi.}$$

From equation (3)

$$\gamma = \frac{1.414F}{bL} = \frac{1.414(30)}{0.35(4)} = 30.3 \text{ ksi.}$$

C. ECCENTRICALLY LOADED MODEL

From data, Table 3 and Fig. 7.

$F = 24$ kips total; 12 kips per strap

$e = 6.5$ inches

$b = 0.35$ inches

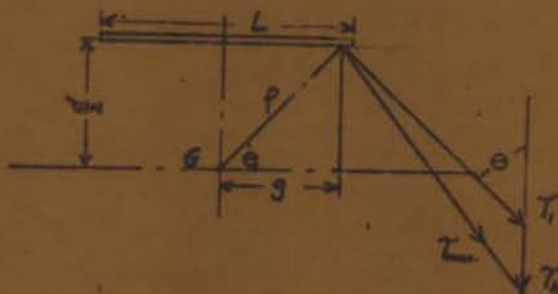
$L = 5$ inches

$d = 5$ inches

$g = 2.25$ inches

$t = 0.248$ inches

For Station 1



The hypotenuse p is; $p = \sqrt{\left(\frac{L}{2}\right)^2 + (g)^2}$

$$p = \sqrt{(2.5)^2 + (2.25)^2} = 3.36 \text{ inches}$$

$$\theta = \sin^{-1} \frac{2.5}{3.36} = 48^\circ$$

The moment of inertia of the weld metal with respect to centroid G is,

$$J_G = 2 \left(\frac{tLd^3}{4} + \frac{tL^3}{12} \right)$$

$$J_G = 2 \left(\frac{0.25(5)(5)^3}{4} + \frac{0.25(5)^3}{12} \right) = 20.6 \text{ inches}^4$$

Using equation (4)

$$\tau_1 = \frac{Fap}{J_G} = \frac{12(6.9)(3.36)}{20.6} = 12.71 \text{ ksi}$$

Using equation (5)

$$\tau_2 = \frac{F}{2tL} = \frac{12}{2(0.25)(5)} = 4.8 \text{ ksi}$$

Adding τ_1 and τ_2 vectorily by means of the law of cosines,

$$\tau_{max}^2 = \tau_1^2 + \tau_2^2 + 2\tau_1\tau_2 \cos \theta$$

$$\tau_{max}^2 = (12.71)^2 + (4.8)^2 + 2(12.71)(4.8) \cos 48^\circ$$

$$\tau_{max} = 16.4 \text{ ksi.}$$

2. Reduction of Data

For the Eccentric Model, Load Eccentricity, e = 8.5 inches

For Station 1

From data, Table 4, plots of load versus strain (see Fig. 11, page 61 for typical plots) were made for each element of the rosette. From these plots the slope of the loading curve provides:

$$\text{For gage elements a : } \frac{493 \text{ microinches per inch}}{16 \text{ kips}}$$

$$b : \frac{-347 \text{ microinches per inch}}{16 \text{ kips}}$$

$$c : \frac{585 \text{ microinches per inch}}{16 \text{ kips}}$$

Thus for a load of 16 kips (9 kips per strap) the strains are,

$$= \frac{16}{16} \times 493 = 544 \text{ microinches per inch}$$

$$= \frac{16}{16} \times (-347) = -390 \text{ microinches per inch}$$

$$= \frac{16}{16} \times 585 = 658 \text{ microinches per inch}$$

Using the standard equations for a 60 degree rosette, given by Timoshenko /10/, and others,

$$m = \frac{\epsilon_a + \epsilon_b + \epsilon_c}{3} = \frac{544 + (-390) + 658}{3} = 274 \text{ microinches per inch}$$

$$r^2 = (\epsilon_a - m)^2 + \left(\frac{\epsilon_c - \epsilon_b}{\sqrt{3}} \right)^2$$

$$r = \left[(544 - 274)^2 + \left(\frac{658 - (-390)}{\sqrt{3}} \right)^2 \right]^{1/2} = 665 \text{ microinches per inch}$$

$$\theta = \frac{1}{2} \tan^{-1} \frac{(E_1 - E_2)(\nu)}{(E_2 - m)} = \frac{1}{2} \tan^{-1} \frac{(800 - 10)(15)}{(55 - 374)} = 32.55^\circ$$

$$e_1 = m + r = 274 + 665 = 939 \text{ microinches per inch}$$

$$e_2 = m - r = 274 - 665 = -391 \text{ microinches per inch}$$

With Poisson's ratio, μ as 0.3 and Young's modulus E as

30×10^6 lbs. per sq. inch and substituting in

$$\sigma_1 = \frac{E}{1 - \mu^2} (e_1 + \mu e_2)$$

$$\sigma_2 = \frac{E}{1 - \mu^2} (e_2 + \mu e_1)$$

$$\gamma_{max} = \frac{1}{2} (\sigma_1 - \sigma_2)$$

$$\sigma_1 = \frac{30 \times 10^6}{1 - (0.3)^2} (939 \times 10^{-6} + 0.3(-391 \times 10^{-6})) = 27.10 \text{ ksi}$$

$$\sigma_2 = \frac{30 \times 10^6}{1 - (0.3)^2} (-391 \times 10^{-6} + 0.3(939 \times 10^{-6})) = -3.59 \text{ ksi}$$

$$\gamma_{max} = \frac{1}{2} (27.10 + 3.59) = 15.35 \text{ ksi}$$

From Mohr's Circle, using x as the direction of the strain in element a , which is along the weld, we get

$$\tau_{xy} = \tau_{max} \sin 2\theta = 15.35 \sin 65.1^\circ = 13.92 \text{ ksi}$$

$$\sigma_x = \sigma_2 + \tau_{max} + \tau_{max} \cos 2\theta$$

$$\sigma_x = -3.59 + 15.35 + 15.35 \cos 65.1^\circ = 18.21 \text{ ksi}$$

$$\sigma_y = \sigma_2 + \tau_{max} - \tau_{max} \cos 2\theta$$

$$\sigma_y = -3.59 + 15.35 - 15.35 \cos 65.1^\circ = 5.31 \text{ ksi.}$$

Strain gage data were reduced by means of a Control Data Corporation 1604 digital computer. Inputs to the data reduction program were ϵ_x , ϵ_y and ϵ_z . Outputs were σ_1 , σ_2 , τ_{max} and θ the angle of orientation of the principal directions relative to the longitudinal axis of the weld. The program, coded in FORTRAN computer language, is shown in Fig. 24, page 75. This program is called "Stress Sixty".

Design calculations for various eccentricities of loadings were done by the 1604 computer. This program, entitled "Design" is shown in Fig. 24, page 75. Inputs were load P , eccentricity e , coordinates of the rosette

stations, and constants determined by modal geometry.

Outputs were χ_{max} and ϕ , the angle of χ_{max} relative to the longitudinal axis of the weld.

APPENDIX B

Subject

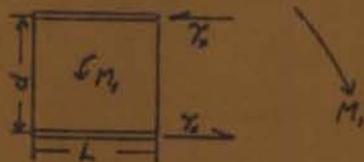
Analysis of Design Method of Eccentrically Loaded weld model by
superposition.

Substituting in equations (4a) and (4b)

$$(6) \tau_c = \frac{\tau_c d}{\sqrt{l^2 + d^2}}$$

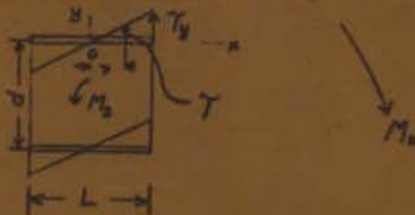
$$(7) \tau_s = \frac{\tau_c L}{\sqrt{L^2 + d^2}}$$

Now consider the mechanisms by which the couple P_e is resisted to be; first, a couple, M_1 , formed by the horizontal shear stress acting along the throat area, tL .



$$(8) M_1 = \tau_c t L d$$

Second, the vertical shear stresses acting across the throat area tL produce a resisting moment, M_2 .



To compute M_2 , consider the moment about the origin of the x-y coordinate system centered on the upper weld. The differential force, dF , is:

$$dF = \tau dA$$

$$dA = t dx$$

$$\tau = \frac{2\tau_y x}{L}$$

$$dF = \frac{2\tau_y x t dx}{L}$$

Since M_2 is four times the moment of dF ,

$$M_2 = 4 \int_0^{L/2} \frac{2\tau_y x^2 t dx}{L}$$

Integrating,

$$(9) \quad M_2 = \frac{\tau_y t L^2}{3}$$

When the moment F_e is replaced by a force F and a couple F_e , the force F is assumed to be resisted by a vertical shear such that:

$$(10) \quad \tau_y d = \frac{F}{A} = \frac{F}{2tL}$$

For equilibrium:

$$(11) \quad F_e = M_1 + M_2$$

Let λ be the fraction of the couple F_e that is resisted by M_1 . Then M_2 must carry $(1-\lambda)$ times F_e .

$$\lambda = \frac{M_1}{F_0} \quad \text{or,}$$

$$(12) \quad \lambda = \frac{M_1}{M_1 + M_2}$$

Substitute from equation (8), page 32 for M_1 , and equation (9), page 31 for M_2 .

$$\lambda = \frac{\bar{\gamma}_x t L d}{\bar{\gamma}_x t L d + \frac{\bar{\gamma}_y t L^2}{3}}$$

Replacing $\bar{\gamma}_x$ and $\bar{\gamma}_y$ by values given in equations (4a) and (4b), page 31, and reducing, λ becomes:

$$(13) \quad \lambda = \frac{d^2}{d^2 + \frac{L^2}{3}}$$

Consider the longitudinal weld model loaded in tension. Assume the horizontal shear stresses along one weld to be reversed.



$$\bar{\gamma}_x = \frac{F_x}{2tL} \quad \text{or} \quad \bar{\gamma}_x t = \frac{F_x}{2L}$$

This is seen to be equivalent to the first resisting mechanism of the design convention. At any point along the weld length, there is a number c_1 , such that

$$\bar{\gamma}_s = c_1 \bar{\gamma}_a = c_1 \frac{F_y}{2tL} \quad \text{or}$$

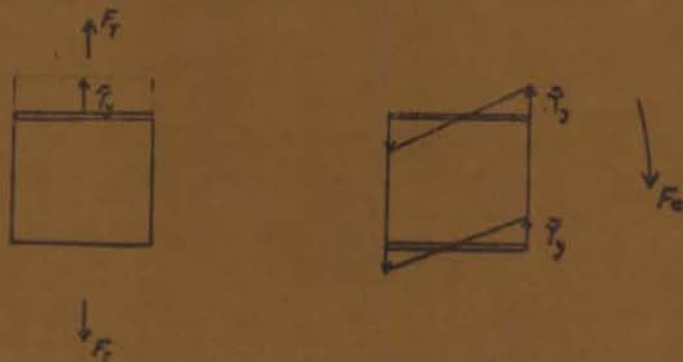
$$(14) \quad \frac{c_1}{t} = \frac{2 \bar{\gamma}_s L}{F_y}$$

$$\text{and} \quad M_1 = \bar{\gamma}_s t L d \quad \text{or} \quad \bar{\gamma}_s = \frac{M_1}{t L d}$$

Substituting for $\bar{\gamma}_s = \frac{\gamma_s}{c_1}$, and rearranging

$$(15) \quad \gamma_s = \frac{c_1 M_1}{t L d}$$

In a similar manner consider the transverse weld model to be loaded in tension. Assume that the average shear stress in the vertical direction is equal to the maximum shear stress the weld incurs in resisting the couple F_y as shown



$$\bar{\gamma}_y = \frac{F_y}{tL}$$

This is equivalent to the second resisting mechanism of the design convention. At any point along the weld there is a number c_2 , such that $\tau_y = c_2 \bar{\tau}_y$ or $\tau_y = c_2 \frac{F_T}{tL}$,

thus

$$(16) \quad \frac{c_2}{t} = \frac{\tau_y L}{F_T}$$

from equation (9), $M_2 = \frac{\bar{\tau}_y t L^2}{3}$ or $\bar{\tau}_y = \frac{3 M_2}{t L^2}$

substituting for $\bar{\tau}_y = \frac{\tau_y}{c_2}$

$$(17) \quad \tau_y = \frac{3 c_2 M_2}{t L^2}$$

For the direct load, from equation (10)

$$\bar{\tau}_{y0} = \frac{F_T}{2tL} \quad \text{also} \quad \tau_{y0} = c_2 \bar{\tau}_{y0}$$

combining

$$(18) \quad \tau_{y0} = \frac{c_2 F_T}{2tL}$$

Let the eccentrically loaded model be loaded. The stresses induced in the welds are caused by:

- 1) resisting with moment M_1 .
- 2) resisting with moment M_2 .
- 3) resisting direct load F .

Designate these stresses τ_x , τ_y and τ_{xy} . By equations (15), (17) and (18),

$$(15) \quad \tau_x = c_1 M_1 / t L d$$

$$(17) \quad \tau_y = 3c_2 M_2 / t L^2$$

$$(18) \quad \tau_{xy} = c_3 F / 2tL$$

Superposing, the total shear stress τ_{xy} in the eccentrically loaded model is

$$(19a) \quad \tau_{xy} = \frac{c_1 M_1}{t L d} + \frac{3c_2 M_2}{t L^2} + \frac{c_3 F}{2tL}$$

Since $M_1 = \lambda Fc$, $M_2 = (1-\lambda)Fc$ as given by equations (12a) and (12b), equation (19a) becomes

$$(19b) \quad \tau_{xy} = \frac{c_1 \lambda Fc}{t L d} + \frac{c_2 (1-\lambda)Fc}{t L^2} + \frac{c_3 F}{2tL}$$

To evaluate the terms c_1/k and c_2/k , experimental data from the longitudinal and transverse model tests will be used in equations (14) and (16) respectively.

Sample Calculations

A set of sample calculations will be shown for a point .0625 of the length of the weld away from the end nearest the load.

The fraction $\lambda = \frac{V_2}{M}$, equation (13), is

$$\lambda = \frac{d^2}{d^2 + \frac{L^2}{3}} = \frac{5.35^2}{5.35^2 + \frac{5^2}{3}} = 0.775$$

where $d = 5.35$ inches, $L = 5$ inches, from Fig. 7.

From tabulated calculations p. 45 and Figs. 3 and 4,
we find these data:

Longitudinal Model

$$\gamma_{xy} = \gamma_x = 14.57 \text{ ksi}$$

$$t = 0.248 \text{ inches}$$

$$L = 4 \text{ inches}$$

$$F_x = 42 \text{ kips}$$

Transverse Model

$$\gamma_{xy} = \gamma_y = 5.45 \text{ ksi}$$

$$t = 0.248 \text{ inches}$$

$$L = 4 \text{ inches}$$

$$F_y = 30 \text{ kips}$$

From equations (14) and (16)

$$(14) \frac{C_1}{t} = \frac{2\gamma_x L}{F_x} = \frac{2(14.57)(4)}{42} = 2.78 \text{ inches}^{-1}$$

$$(16) \frac{C_2}{t} = \frac{\gamma_y L}{F_y} = \frac{5.45(4)}{30} = 0.726 \text{ inches}^{-1}$$

For the eccentrically loaded model from Fig. 7 and data, Table 4, substitute these data.

$$F = 9 \text{ kips}$$

$$e = 8.5 \text{ inches}$$

$$L = 5 \text{ inches}$$

$$d = 5.35 \text{ inches, in equation (19b)}$$

$$\gamma_{xy} = \frac{c_1 \lambda F e}{t L d} + \frac{c_2 (1-\lambda) F e}{t L^2} + \frac{c_3 E}{2 t L} =$$

$$\gamma_{xy} = \frac{2.78 (0.775) (9) (8.5)}{5 (5.35)} + \frac{0.726 (2.25) (9) (8.5)}{(5^2)} + \frac{0.726 (9)}{2 (5)} =$$

$$\gamma_{xy} = 7.97 \text{ ksi.}$$

The experimental value of γ_{xy} at this location was 13.3 ksi.

The values of γ_{xy} computed by the foregoing plan are compared with experimental values for load eccentricity of 8.5 inches in Fig. 22. Since the correlation is very poor, it is concluded that the superposition plan using data from the transverse and longitudinal models is not justified.

TABLE 1

Data for Final Run of Longitudinal Model

Total Load in Kips	STATION 1			STATION 2		
	Strain Indicator Reading in Microinches per Inch			Strain Indicator Reading in Microinches per Inch		
	a	b	c	a	b	c
12	1000	995	999	998	999	999
24	1081	927	1041	1048	971	1035
36	1171	839	1092	1099	941	1078
48	1269	730	1050	1152	892	1138
60	1370	617	1206	1207	830	1215
72	1470	501	1268	1262	766	1289
84	1565	388	1326	1318	704	1365
96	1678	248	1448	1302	670	1554

Total Load in Kips	STATION 3			STATION 4		
	Strain Indicator Reading in Microinches per Inch			Strain Indicator Reading in Microinches per Inch		
	a	b	c	a	b	c
12	1000	993	995	997	995	999
24	1049	975	1020	1010	1000	1028
36	1094	955	1049	1023	1009	1060
48	1132	924	1091	1035	1015	1100
60	1192	884	1154	1050	1019	1052
72	1241	840	1220	1065	1020	1209
84	1290	800	1281	1078	1021	1260
96	1288	685	1455	1216	560	1388

$$\text{Load Per Strap} = \frac{\text{total load}}{2}$$

TABLE 2

Data for Final Run of Transverse Model

Total Load in Kips	STATION 1			STATION 2		
	Strain Indicator Reading in Microinches per Inch			Strain Indicator Reading in Microinches per Inch		
	a	b	c	a	b	c
6	1000	1000	1000	1000	1000	1000
18	969	1236	1152	972	1230	1121
24	942	1365	1242	960	1349	1189
30	922	1498	1330	949	1470	1256
36	901	1629	1418	936	1592	1321
42	880	1752	1500	914	1709	1387
48	862	1876	1585	899	1823	1450
54	842	1998	1665	885	1938	1518
60	822	2135	1738	872	2068	1581

Total Load in Kips	STATION 3			STATION 4		
	Strain Indicator Reading in Microinches per Inch			Strain Indicator Reading in Microinches per Inch		
	a	b	c	a	b	c
6	1000	1000	1000	1000	1000	1000
18	971	1233	1102	959	1171	1270
24	960	1348	1155	940	1250	1400
30	947	1468	1210	920	1335	1538
36	934	1579	1261	901	1419	1673
42	920	1698	1312	880	1496	1802
48	907	1808	1362	862	1574	1933
54	894	1921	1414	842	1658	2073
60	880	2045	1460	822	1740	2201
66	867	2175	1504	798	1830	2347

Load Per Strap = $\frac{\text{total load}}{2}$

TABLE 3

Data for Final Run of Eccentrically Loaded Model.
Load Eccentricity, $e = 6.5$ inches

Total Load in Kips	STATION 1			STATION 2		
	Strain Indicator Reading in Microinches per Inch			Strain Indicator Reading in Microinches per Inch		
	a	b	c	a	b	c
2	1000	1000	1000	1000	1000	1000
6	1094	949	1114	1068	989	1024
12	1229	869	1285	1161	970	1060
18	1360	781	1451	1266	948	1100
24	1492	685	1628	1352	913	1142
18	1358	760	1460	1262	928	1113
12	1228	845	1302	1171	947	1080
6	1098	930	1130	1075	970	1038
2	1002	999	1001	1000	999	1000

Total Load in Kips	STATION 3			STATION 4		
	Strain Indicator Reading in Microinches per Inch			Strain Indicator Reading in Microinches per Inch		
	a	b	c	a	b	c
2	1000	1000	1000	1000	1000	1000
6	1070	992	1012	1029	969	1038
12	1165	982	1028	1063	921	1085
18	1253	970	1045	1097	872	1130
24	1342	952	1068	1138	800	1180
18	1255	960	1055	1105	850	1142
12	1164	970	1040	1072	898	1100
6	1072	982	1021	1037	948	1050
2	1001	999	1000	1007	986	1000

$$\text{Load Per Strap} = \frac{\text{total load}}{2}$$

TABLE 4

Data for Final Run of Eccentrically Loaded Model
Load Eccentricity, $e = 8.5$ inches

Total Load in Kips	STATION 1			STATION 2		
	Strain Indicator Reading in Microinches per Inch			Strain Indicator Reading in Microinches per Inch		
	a	b	c	a	b	c
2	1000	1000	1000	1000	1000	1000
6	1128	920	1141	1084	986	1029
10	1250	840	1283	1167	970	1053
14	1374	750	1430	1248	951	1085
18	1493	653	1585	1331	925	1120
14	1370	730	1444	1252	935	1100
10	1252	811	1312	1176	949	1073
6	1130	900	1169	1095	970	1043
2	1001	1001	1002	1000	1000	1000

Total Load in Kips	STATION 3			STATION 4		
	Strain Indicator Reading in Microinches per Inch			Strain Indicator Reading in Microinches per Inch		
	a	b	c	a	b	c
2	1000	1000	1000	1000	1000	1000
6	1079	995	1010	1029	960	1036
10	1190	989	1019	1055	918	1063
14	1220	982	1029	1080	879	1097
18	1299	974	1041	1103	838	1130
14	1220	977	1036	1081	872	1101
10	1190	980	1028	1056	911	1075
6	1080	989	1020	1030	951	1043
2	1000	1000	1001	998	999	1000

$$\text{Load Per Strip} = \frac{\text{total load}}{2}$$

TABLE 5

Data for Final Run of Eccentrically Loaded Model
Load Eccentricity, $e = 10.5$ inches

Total Load in Kips	STATION 1			STATION 2		
	Strain Indicator Reading in Microinches per Inch			Strain Indicator Reading in Microinches per Inch		
	a	b	c	a	b	c
1	1000	1000	1000	1000	1000	1000
4	1123	920	1135	1081	986	1023
7	1242	838	1269	1160	971	1049
10	1365	744	1411	1239	951	1078
13	1481	649	1558	1320	924	1109
10	1362	726	1429	1244	935	1089
7	1248	808	1304	1170	948	1068
4	1129	897	1164	1091	969	1039
1	1000	1001	1002	1000	1000	1000

Total Load in Kips	STATION 3			STATION 4		
	Strain Indicator Reading in Microinches per Inch			Strain Indicator Reading in Microinches per Inch		
	a	b	c	a	b	c
1	1000	1000	1000	1000	1000	1000
4	1072	994	1008	1029	961	1031
7	1141	989	1015	1053	921	1059
10	1208	982	1023	1079	883	1089
13	1269	974	1034	1100	848	1120
10	1206	978	1029	1080	882	1093
7	1141	981	1021	1058	921	1069
4	1077	989	1013	1033	959	1040
1	1000	1000	1000	1002	1003	1000

$$\text{Load Per Strap} = \frac{\text{Total Load}}{2}$$

TABLE 6

Experimental Values of Stress (ksi) for Final Run of Longitudinal
Model for Total Load of 84 Kips or 41 Kips Per Strap

	STATION 1	STATION 2	STATION 3	STATION 4
σ_x	24.0	17.99	14.98	9.98
σ_y	-14.5	-4.94	-2.27	2.48
τ_{xy}	19.3	11.47	8.62	3.75
σ_z	24.5	31.8	29.7	24.1
σ_x	17.45	11.67	10.73	5.06
σ_y	-7.85	1.37	1.97	7.39
τ_{xy}	14.57	10.25	7.41	3.56

TABLE 7

Experimental Values of Stress (ksi) for Final Run of Transverse
Model for Total Load of 60 Kips or 30 Kips Per Strap

	STATION 1	STATION 2	STATION 3	STATION 4
σ_x	46.8	41.9	39.3	49.0
σ_y	7.19	6.56	4.68	7.12
τ_{xy}	19.81	17.66	17.32	20.96
σ_z	8.0	11.4	14.9	-9.6
σ_x	7.96	7.94	7.00	8.27
σ_y	46.02	40.5	36.99	47.89
τ_{xy}	5.45	6.84	6.60	6.87

TABLE 8

Experimental Values of Stress (ksi) for Final Run of Eccentric Model
 Load Eccentricity, $e = 6.5$ Inches, Total Load = 24 Kips
 Load Per Strap = 12 Kips

	STATION 1	STATION 2	STATION 3	STATION 4
σ_1	27.37	12.68	11.46	7.90
σ_2	-2.28	-0.110	-0.178	-4.21
T_{max}	14.82	6.40	5.82	6.05
θ	33.8	15.3	8.41	32.8
σ_3	18.16	11.80	11.20	4.33
σ_4	6.92	0.78	0.12	-0.65
T_y	13.70	3.26	1.68	5.51

TABLE 9

Experimental Values of Stress (ksi) for Final Run of Eccentric Model
 Load Eccentricity, $e = 8.5$ Inches, Total Load = 18 Kips
 or 9 Kips Per Strap

	STATION 1	STATION 2	STATION 3	STATION 4
σ_1	27.10	12.12	9.86	5.97
σ_2	-3.59	-0.043	-0.088	-3.69
T_{max}	15.35	6.08	4.97	4.83
θ	32.5	14.4	5.8	32.4
σ_3	18.21	11.37	9.77	3.19
σ_4	5.31	0.71	-0.01	-0.91
T_y	13.92	2.92	1.0	4.36

TABLE 10

Experimental Values of Stress (ksi) for Final Run of Eccentric Modal
 Load Eccentricity, $e = 10.5$ Inches, Total Load = 12 Kips
 Load Per Strap = 6 Kips

	STATION 1	STATION 2	STATION 3	STATION 4
σ_1	23.24	10.35	8.26	5.02
σ_2	-3.61	-0.211	-0.228	-3.30
τ_{max}	13.42	5.28	4.24	4.16
e	32.2	13.8	5.51	31.8
σ_3	15.61	9.75	8.17	2.71
σ_4	4.01	0.39	-0.15	-0.99
τ_{xy}	12.10	2.45	0.81	3.72

TABLE 11

Comparison of Maximum Shear Stress and Angle of Orientation of Principal Axis for Turning Center at O and Various Values of O' , for Load Eccentricity, $e = 6.5$ Inches

Turning Center at O

	STATION 1	STATION 2	STATION 3	STATION 4
$T_{max. calc.}$	16.36	12.18	9.67	10.14
$T_{max. exp.}$	14.82	6.40	5.82	6.05
$T_{max. calc. / T_{max. exp.}$	0.748	1.27	1.11	1.12
$\theta_{calc.}$	9.6	-5.9	-33.1	23.8
$\theta_{exp.}$	33.8	15.3	8.42	32.8

Turning Center at O' (.75 inches from O)

	STATION 1	STATION 2	STATION 3	STATION 4
$T_{max. calc.}$	20.50	15.40	11.60	10.68
$T_{max. exp.}$	14.82	6.40	5.82	6.05
$T_{max. calc. / T_{max. exp.}$	0.921	1.60	1.33	1.175
$\theta_{calc.}$	13.9	1.5	-20.4	36.9
$\theta_{exp.}$	33.8	15.3	8.42	32.8

Turning Center at O' (.50 inches from O)

	STATION 1	STATION 2	STATION 3	STATION 4
$T_{max. calc.}$	18.40	13.71	10.52	10.05
$T_{max. exp.}$	14.82	6.40	5.82	6.05
$T_{max. calc. / T_{max. exp.}$	0.829	1.43	1.21	1.11
$\theta_{calc.}$	12.9	0.25	-23.5	33.1
$\theta_{exp.}$	33.8	15.3	8.42	32.8

Turning Center at O' (1 inch from O)

	STATION 1	STATION 2	STATION 3	STATION 4
$T_{max. calc.}$	21.92	16.58	12.40	11.28
$T_{max. exp.}$	14.82	6.40	5.82	6.05
$T_{max. calc. / T_{max. exp.}$	0.985	1.73	1.42	1.24
$\theta_{calc.}$	15.1	3.8	-16.5	30.5
$\theta_{exp.}$	33.8	15.3	8.42	32.8

TABLE 12

Comparison of Maximum Shear Stresses (ksi) and Angle of Orientation of Principal Axis for Turning Center at O and O', for Load Eccentricity, $e = 8.5$ Inches

Turning Center at O

	STATION 1	STATION 2	STATION 3	STATION 4
<i>Y_{max} act.</i>	15.15	11.28	9.31	10.4
<i>Y_{max} exp.</i>	15.35	6.08	4.97	4.83
<i>Y_{max} act./Y_{max} exp.</i>	0.656	1.24	1.25	1.44
<i>θ_{act.}</i>	7.3	-10.3	-39.8	18.0
<i>θ_{exp.}</i>	32.5	14.4	5.8	32.4

Turning Center at O' (1.0 inches from O)

	STATION 1	STATION 2	STATION 3	STATION 4
<i>Y_{max} act.</i>	20.1	15.01	11.36	10.50
<i>Y_{max} exp.</i>	15.35	6.08	4.97	4.83
<i>Y_{max} act./Y_{max} exp.</i>	0.873	1.65	1.52	1.45
<i>θ_{act.}</i>	13.8	1.5	-20.8	36.5
<i>θ_{exp.}</i>	32.5	14.4	5.8	32.4

TABLE 13

Comparison of Maximum Shear Stress (ksi) and Angle of Orientation of Principal Axis for Turning Center at O and O' , for Load Eccentricity, $e = 10.5$ Inches

Turning Center at O

	STATION 1	STATION 2	STATION 3	STATION 4
$T_{max. ext.}$	12.03	8.97	7.63	8.84
$T_{max. int.}$	13.42	5.28	4.24	4.16
$T_{max. ext.} / T_{max. int.}$	0.897	1.73	1.80	1.41
$\theta_{ext.}$	5.6	-13.4	-4.5	14.7
$\theta_{int.}$	32.2	13.8	5.5	31.8

Turning Center at O' (1.25 inches from O)

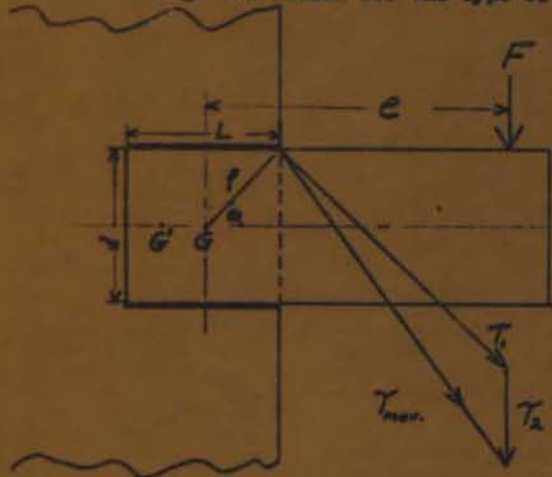
	STATION 1	STATION 2	STATION 3	STATION 4
$T_{max. ext.}$	16.80	12.60	9.52	8.60
$T_{max. int.}$	13.42	5.28	4.24	4.16
$T_{max. ext.} / T_{max. int.}$	0.835	1.59	1.50	1.38
$\theta_{ext.}$	14.3	2.2	-19.3	36.4
$\theta_{int.}$	32.2	13.8	5.5	31.8

TABLE 24

Eccentricity "e" inches	6.5	8.5	10.5	average
Load in kips	12	9	6	
T_{\max} calc., ksi	16.4	15.1	12.0	
T_{\max} exp., ksi	14.82	13.9	13.4	
T_{ave} calc., ksi	11.5	10.9	8.8	
T_{ave} exp., ksi	6.9	6.3	5.8	
$\frac{T_{\text{ave calc.}}}{T_{\text{ave exp.}}}$	1.67	1.73	1.52	1.64
$\frac{T_{\text{ave calc.}}}{1.5T_{\text{ave exp.}}}$	1.116	1.155	1.011	1.09
$\frac{T_{\max \text{ calc.}}}{T_{\text{ave exp.}}}$	1.108	1.086	0.895	1.03
$\frac{T_{\max \text{ calc.}}}{1.5T_{\max \text{ exp.}}}$	0.739	0.723	0.596	0.654

Figure 1

Design Convention for One Type of Eccentrically Loaded Weld



Symbols

- γ - shear stress
- F - Load
- e - eccentricity
- L - weld length
- d - distance between welds
- G - centroid of welds
- f - distance; centroid to point on weld
- t - throat dimension of weld
- θ - an angle
- J - moment of inertia

Conventional Design Equations

$$\tau_1 = \frac{F_0}{J_0}$$

$$\tau_2 = \frac{F}{L} = \frac{F}{2tL}$$

$$\tau_{max} = \tau_1 + \tau_2$$

$$J_0 = 2tL \left(\frac{d^2}{8} + \frac{L^2}{12} \right)$$

Figure 2

Photograph of longitudinally Loaded Weld Model



Figure 3

Sketch of Longitudinally Loaded Weld Model

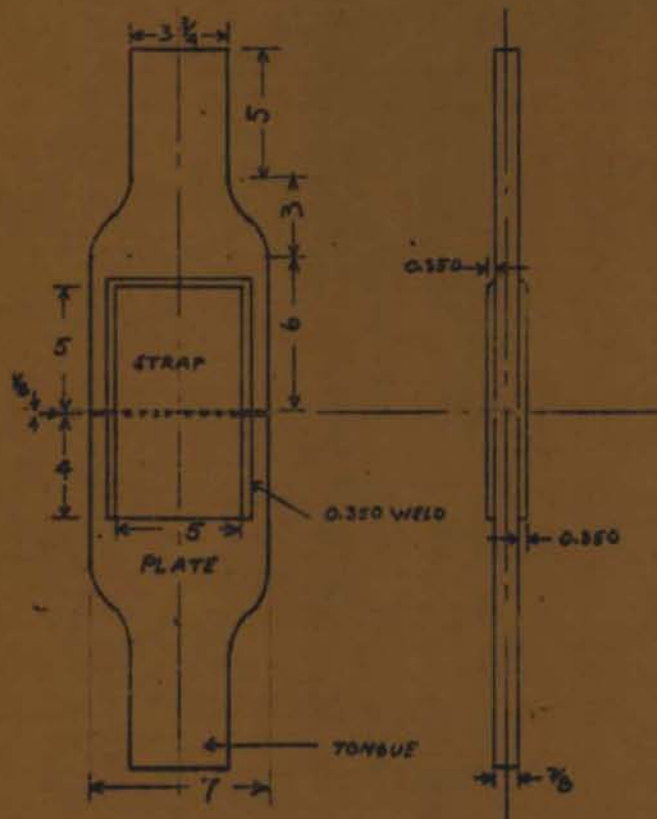


Figure 4

Photograph of Transversely Loaded Weld Model



Figure 6

Photograph of Eccentrically Loaded Weld Model

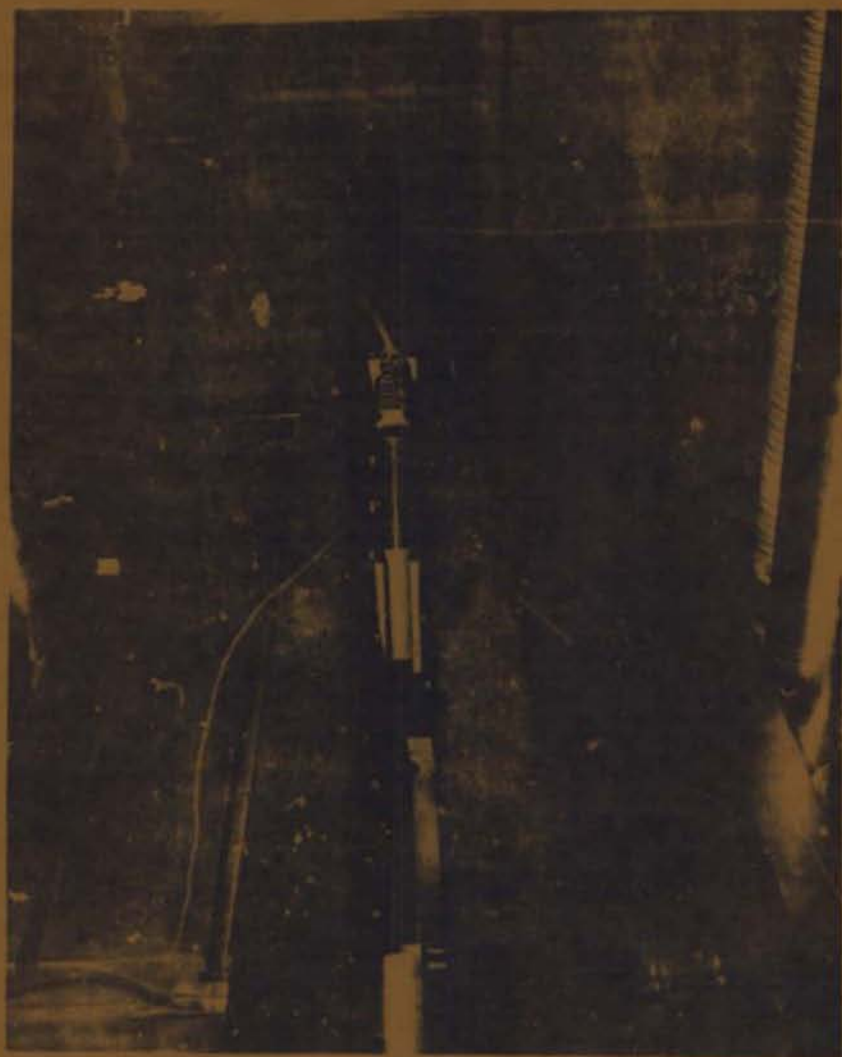


Figure 7

Sketch of Eccentrically Loaded Weld Model

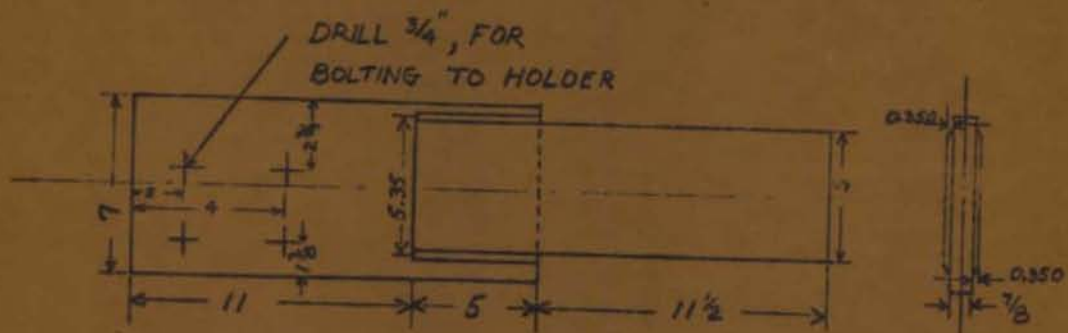
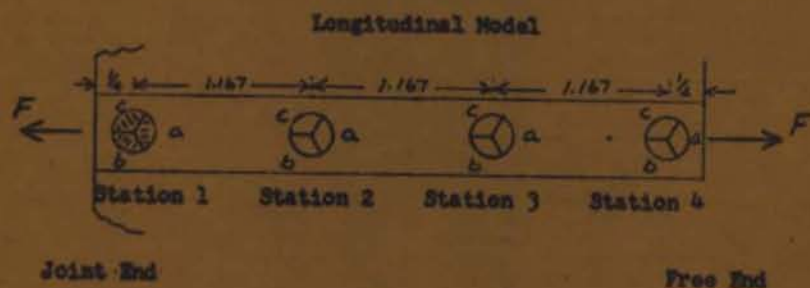


Figure 8

Diagram of Strain-Gage Placement



Joint End

Free End

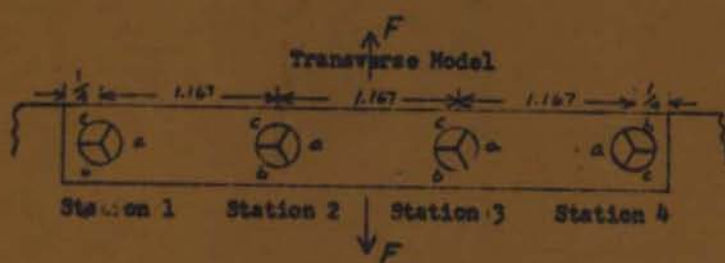


Figure 9

Typical Load-Versus-Strain Plot -
Preliminary Run

Element "b" of Rosette
at Station 1
Longitudinal Model

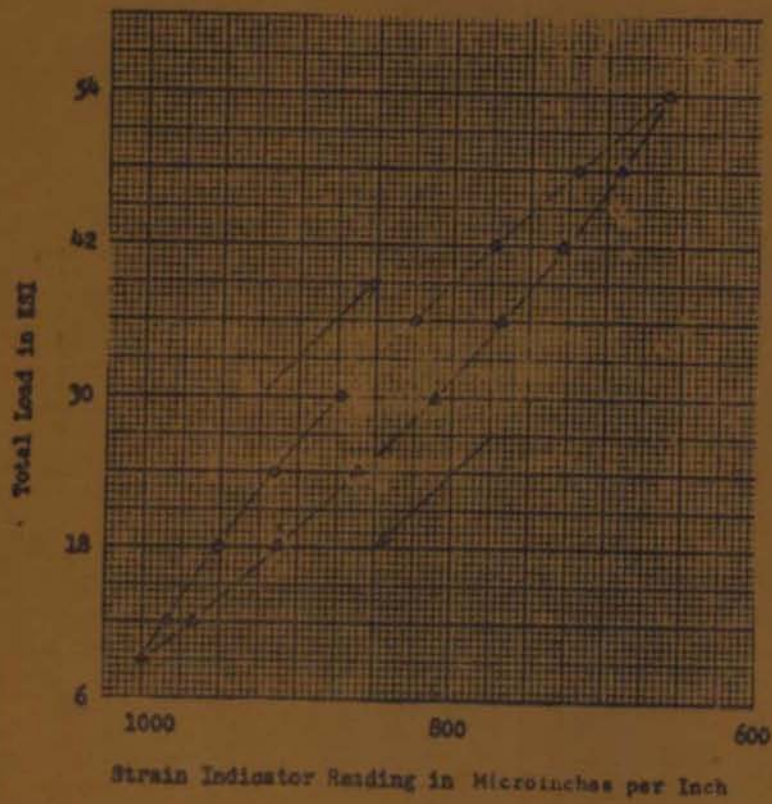


Figure 10

Load-Versus-Strain Plot Showing Hysteresis
Loop Cycles

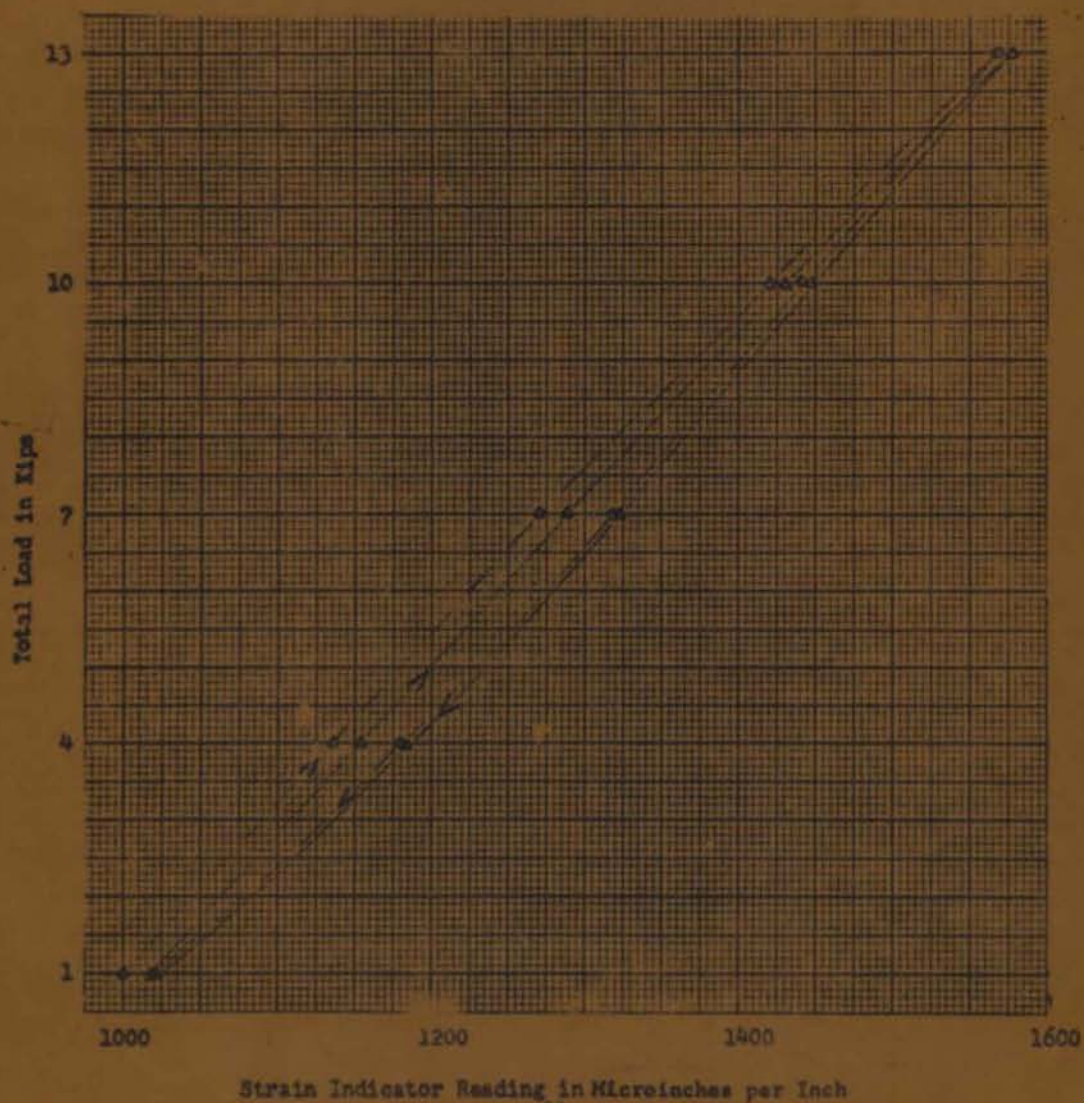


Figure 11

Typical Load-Versus-Strain Plot - Final Run

Longitudinal Model
Station 1
Element "a"

Transverse Model
Station 1
Element "c"

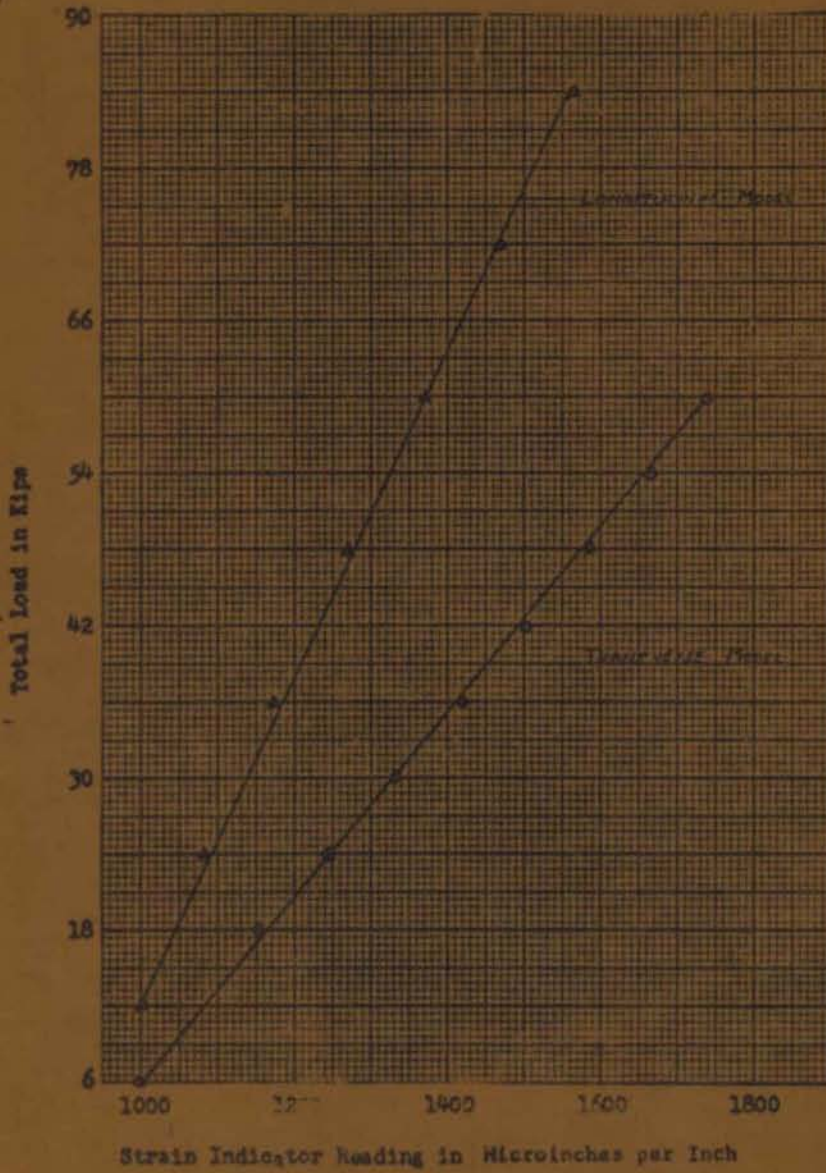


Figure 12
Photograph of Potentially Loaded Model and
Binding Tape on Tooling Machine

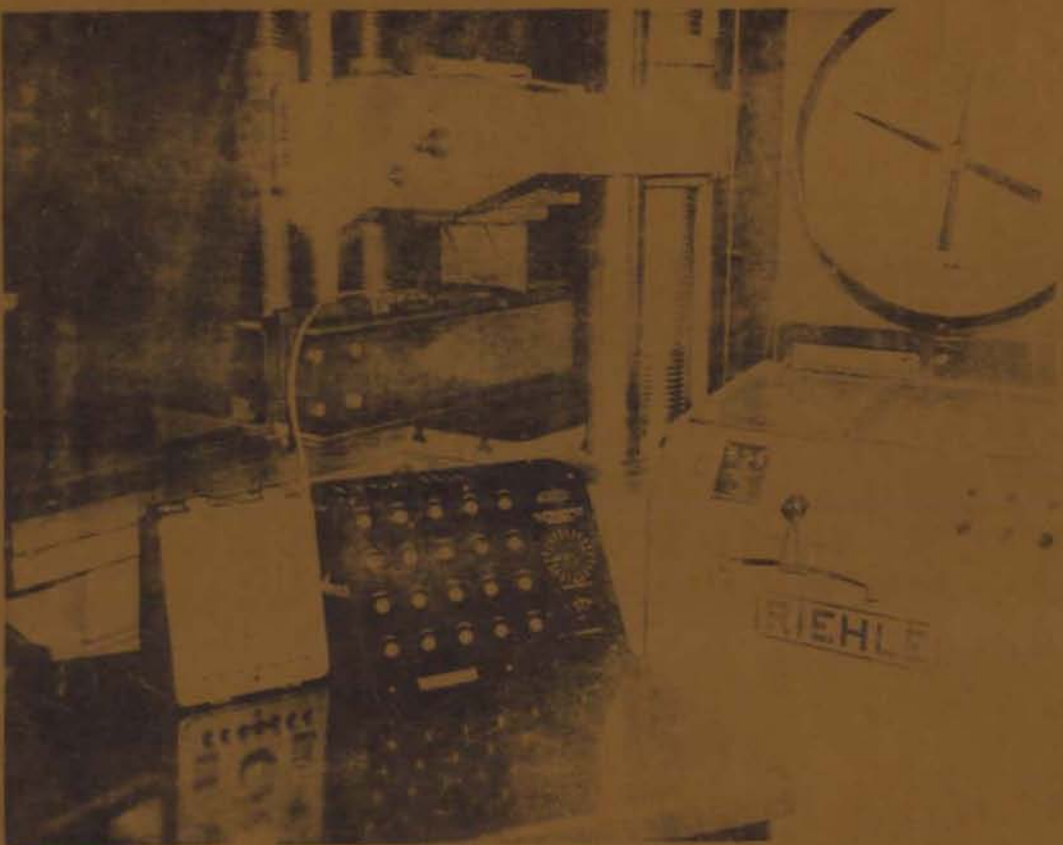


Figure 13
Photograph of Eccentrically Loaded Rods and
Holding Assembly on Testing Machine

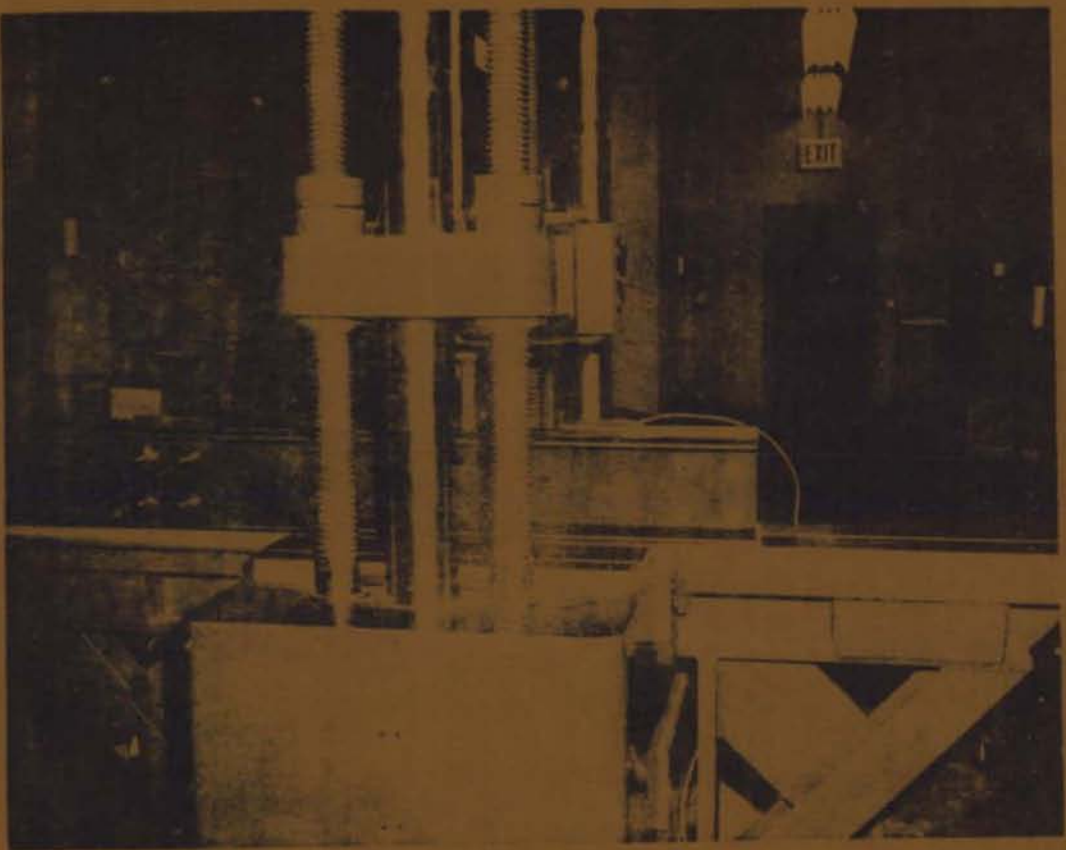


Figure 14

Results of Tests of Longitudinally Loaded Weld

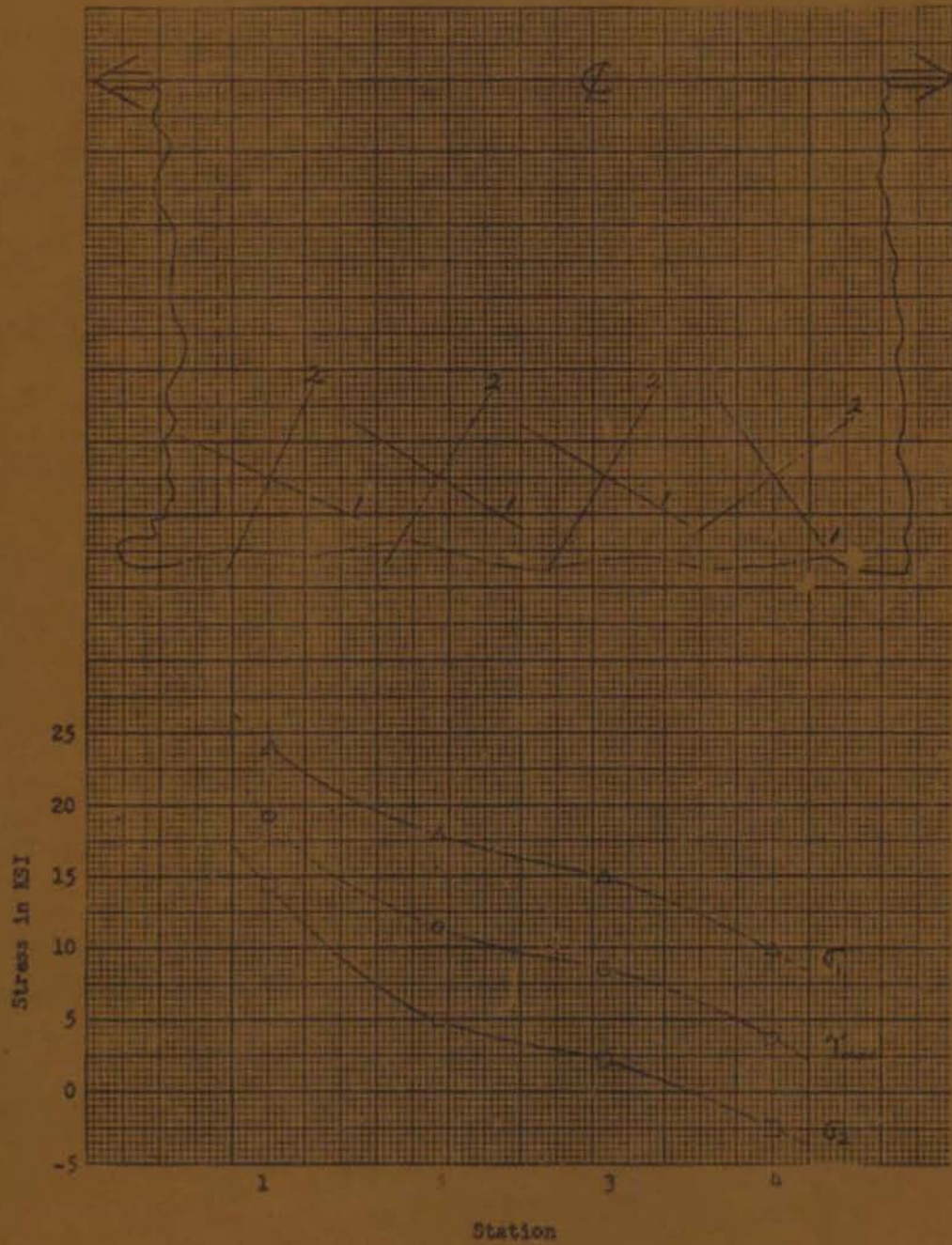
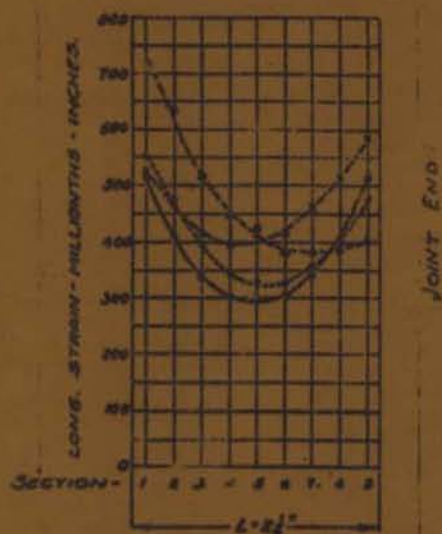


Figure 15

Plot of Load Versus Strain for Longitudinally Loaded Fillet Weld (From Smith/6/)

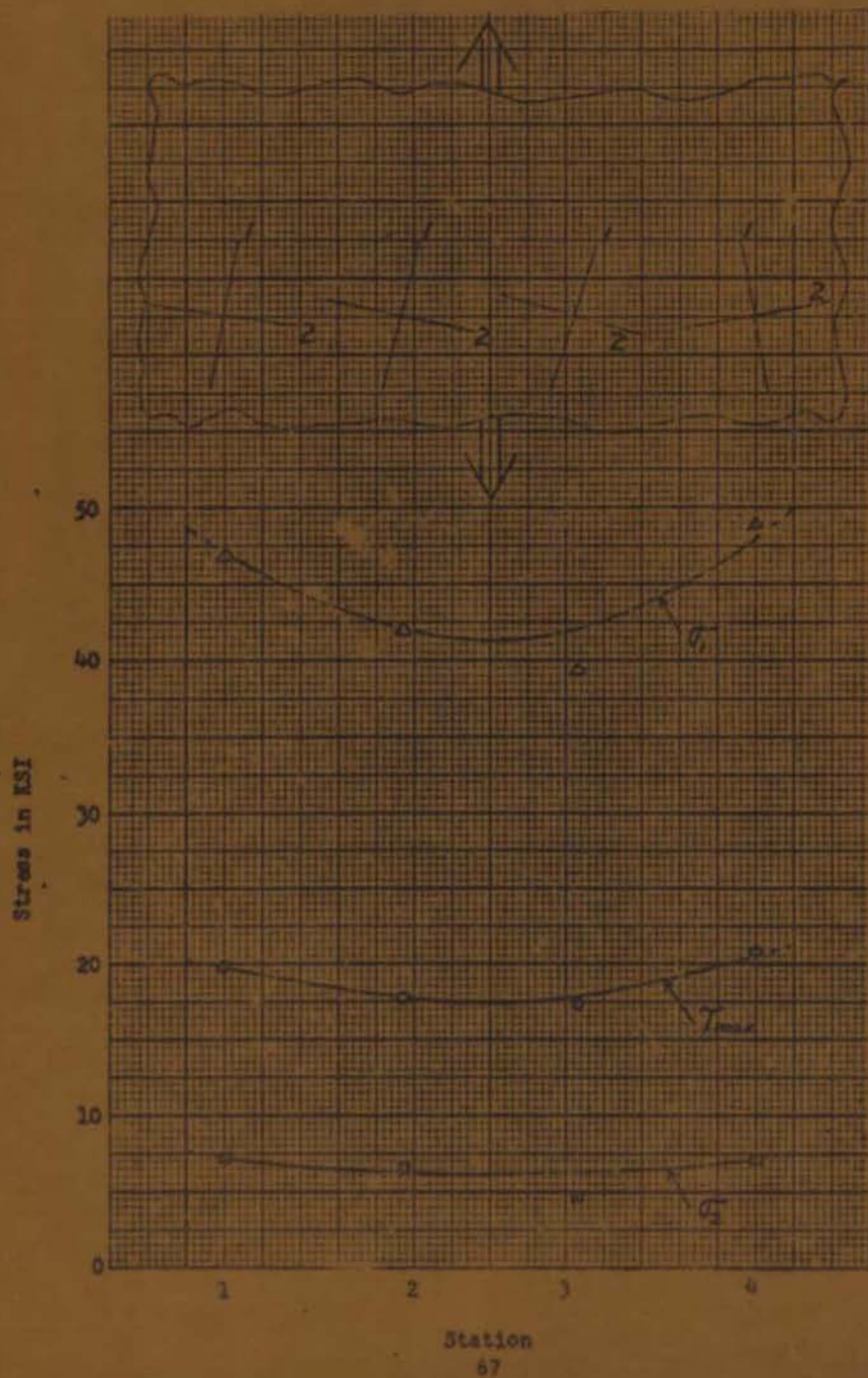


COMPARISON OF CURVES SHOWING CHARACTERISTIC VALUES
LOAD PER WELD, $P = 4000$ POUNDS.

SPECIMEN	GRP BARS	JOINT BARS	R/R_1
→ 3A	$3 \times \frac{1}{2}$ "	$2 \times \frac{3}{8}$ "	1.00
→ 1B	$3 \times \frac{1}{8}$ "	$2 \times \frac{1}{8}$ "	.75
→ 1C	$3 \times \frac{1}{8}$ "	$2 \times \frac{3}{8}$ "	.50
→ 2D	$6 \times \frac{1}{8}$ "	$4 \times \frac{3}{8}$ "	1.00

Figure 16

Results of Test of Transversely Loaded Weld



Station

Figure 17

Results of Test of Eccentrically Loaded Fillet
Weld for Load Eccentricity of 6.5 Inches

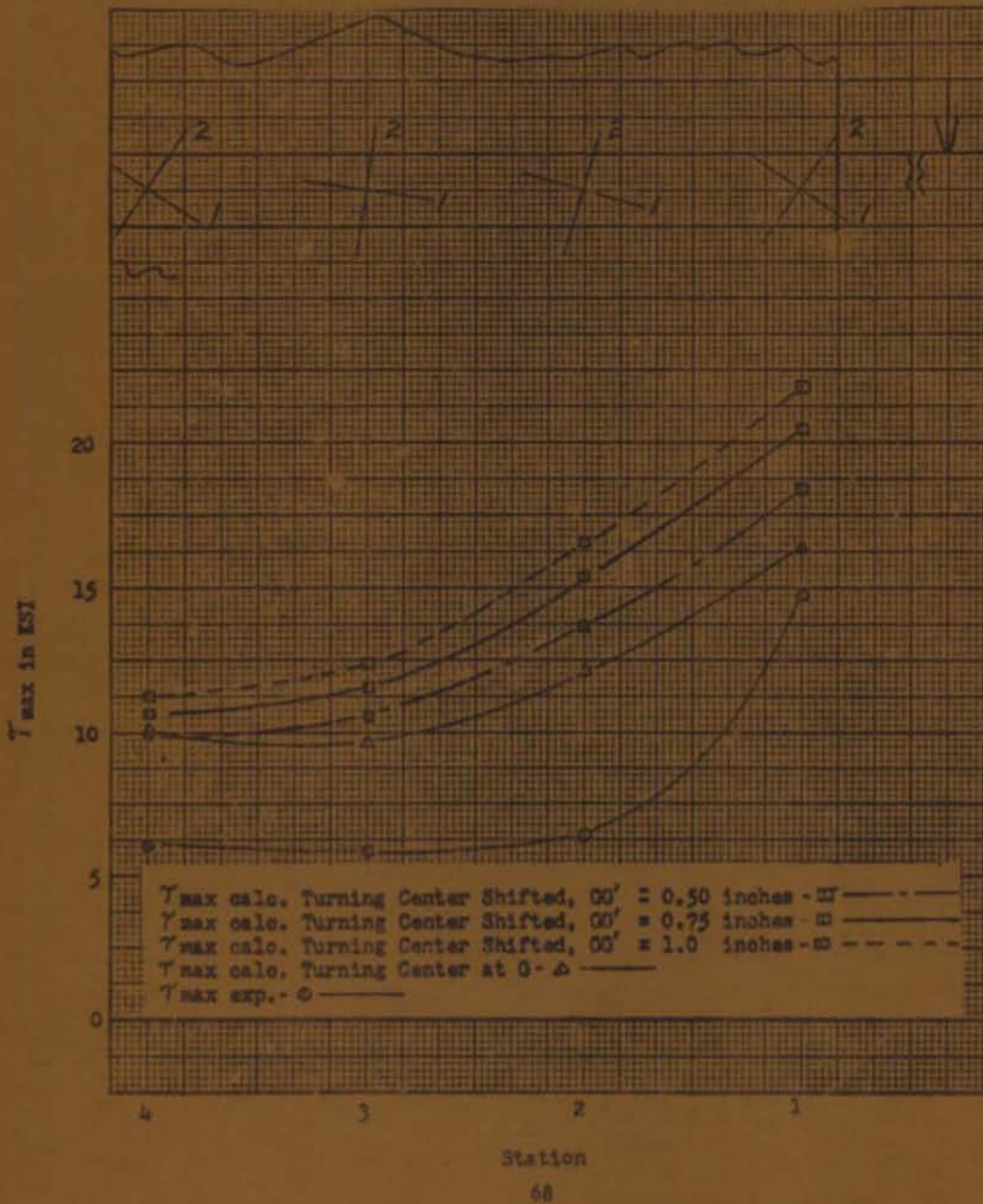


Figure 13

Results of Test of Eccentrically Loaded Fillet
Weld for Load Eccentricity of 8.5 Inches

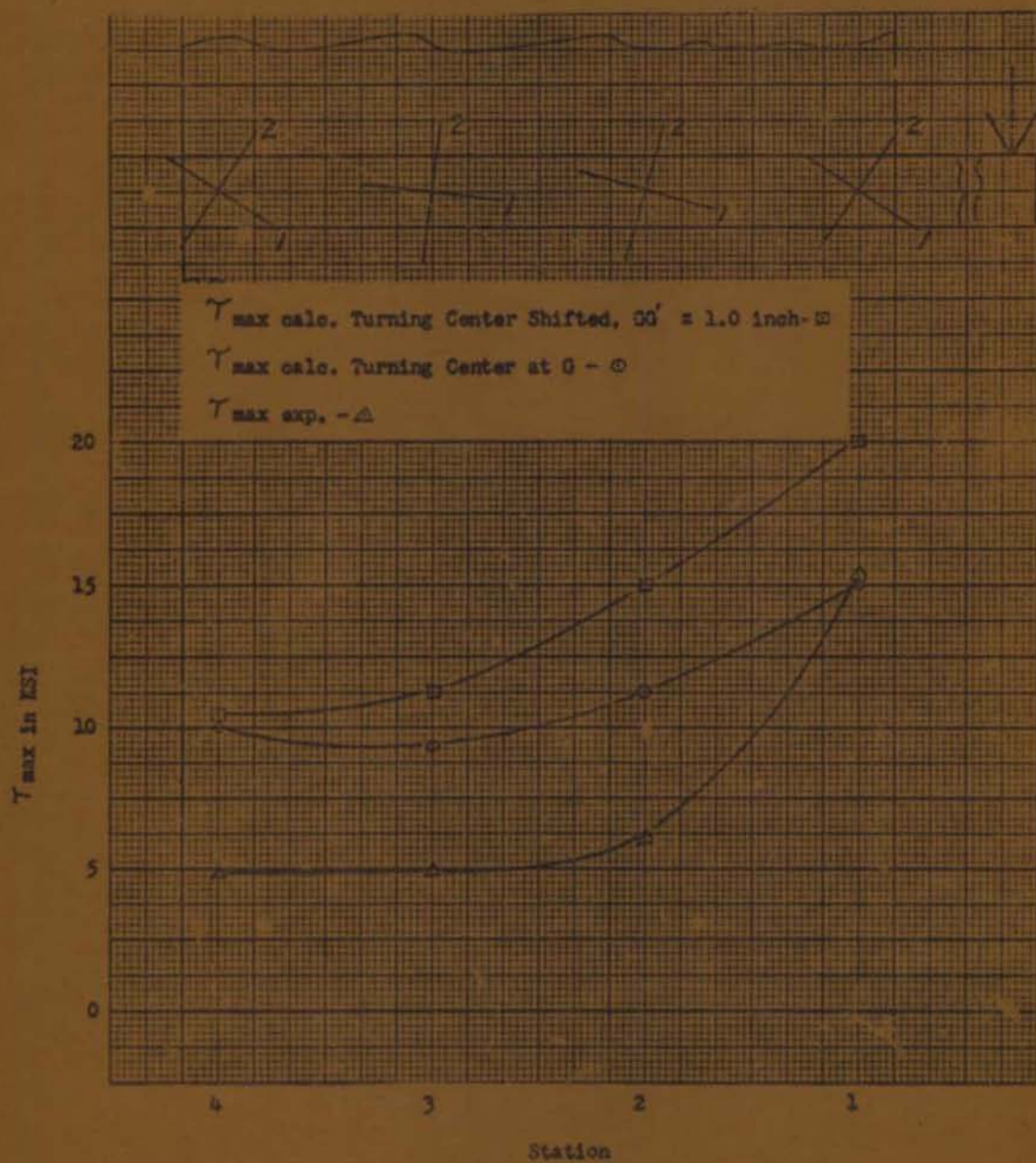


Figure 19

Results of Test of Eccentrically Loaded Fillet Weld
for Load Eccentricity of 10.5 Inches

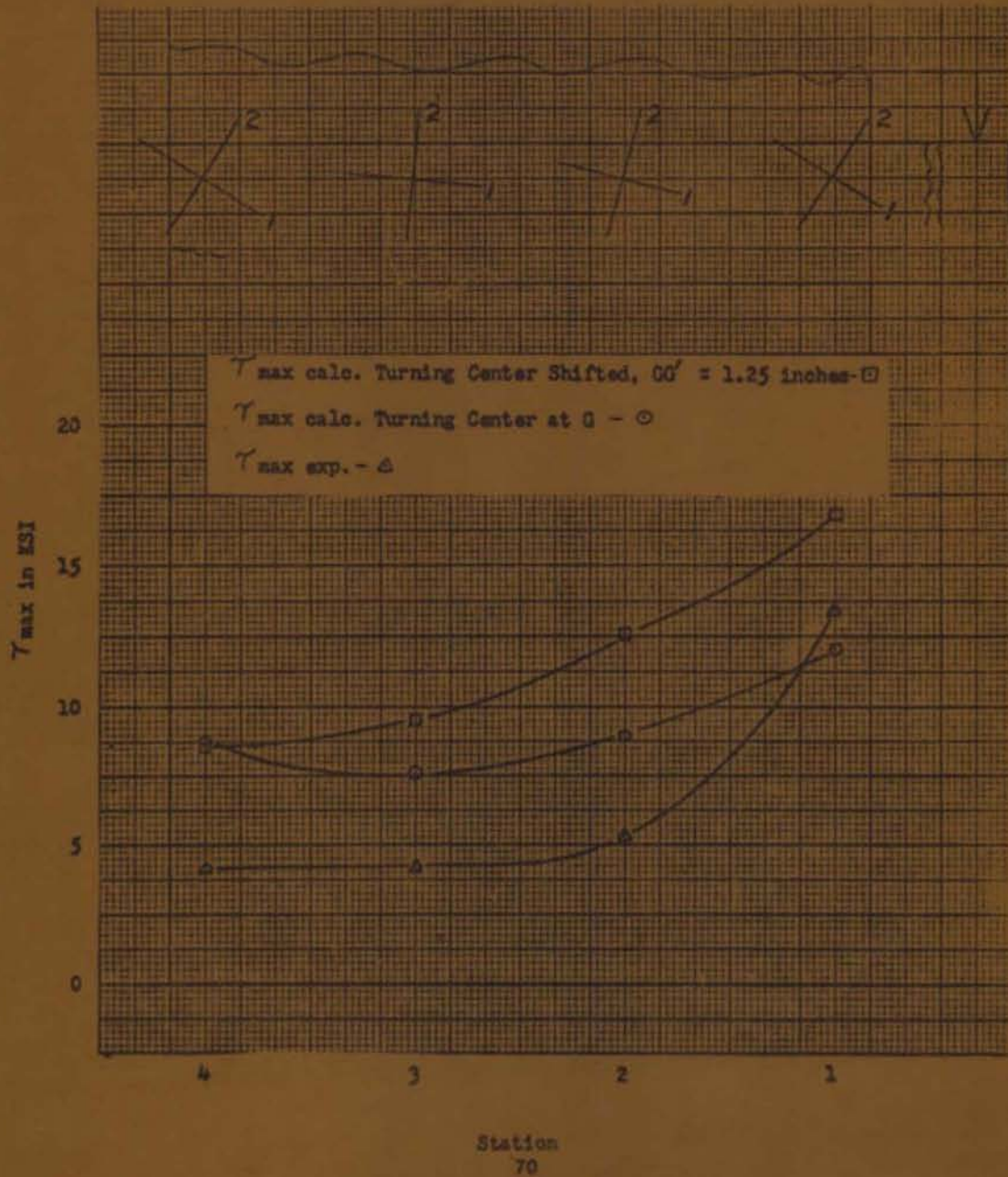


Figure 20

σ_x Stress Distribution for Eccentrically Loaded Fillet Weld

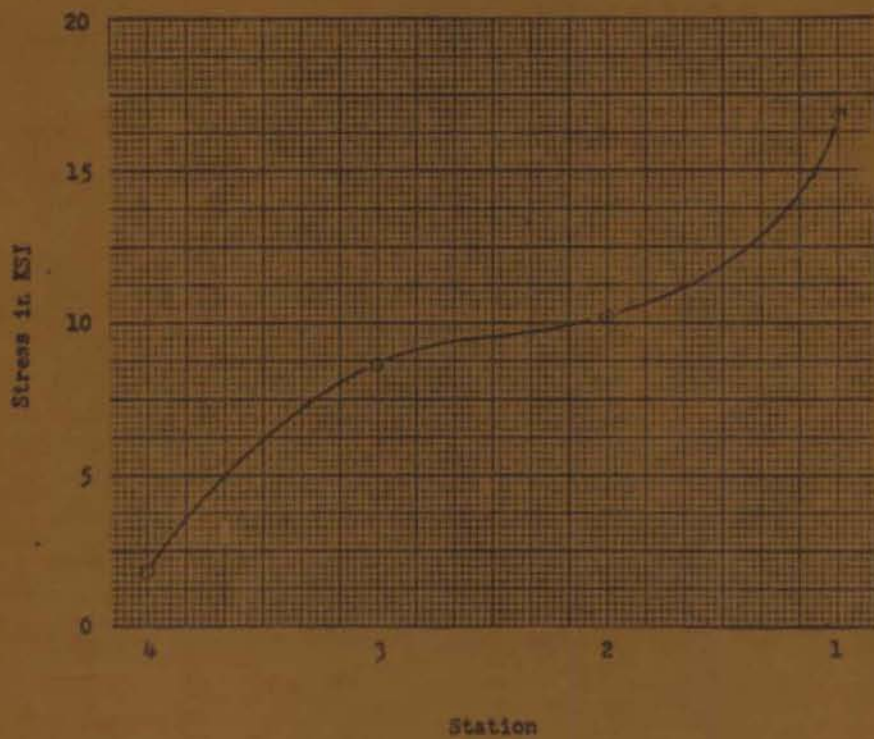


Figure 21

σ_y Stress Distribution for Eccentrically Loaded Fillet Weld

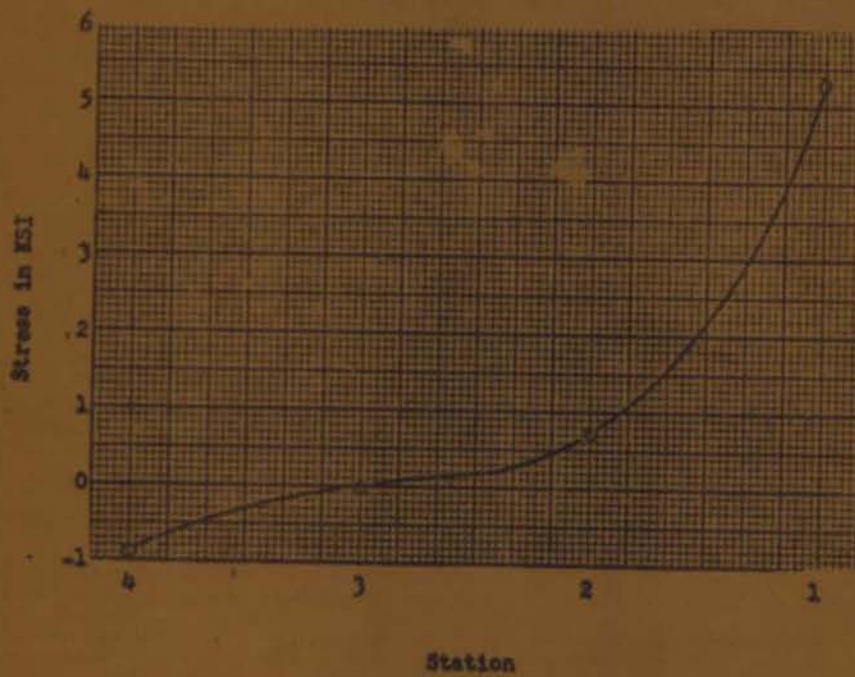


Figure 22

T_{xy} Stress Distribution for Eccentrically Loaded Fillet Weld

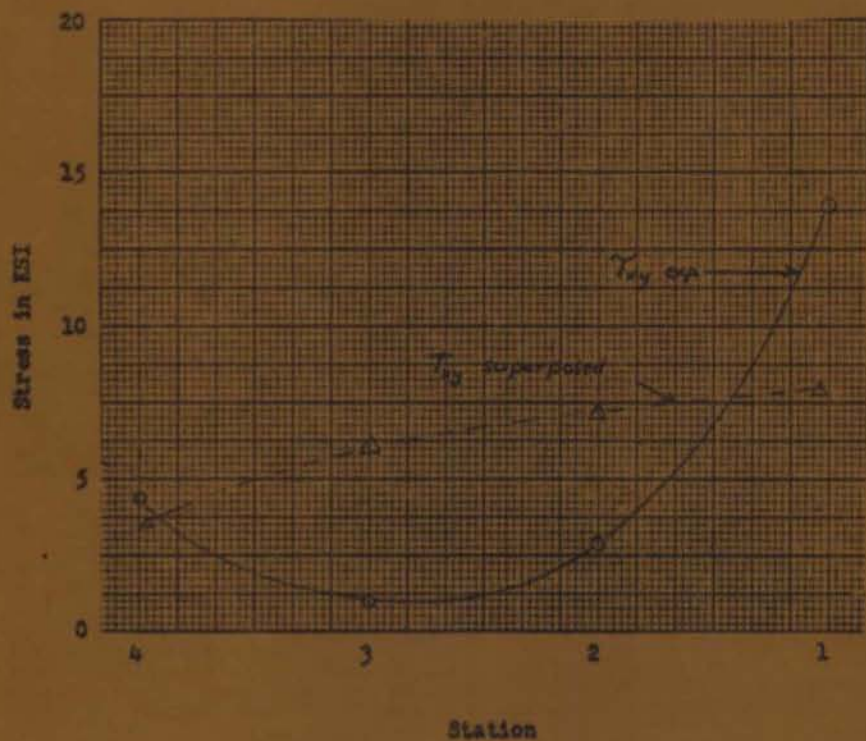


Figure 23

Plot of Load Eccentricity Versus Shift of Turning Center

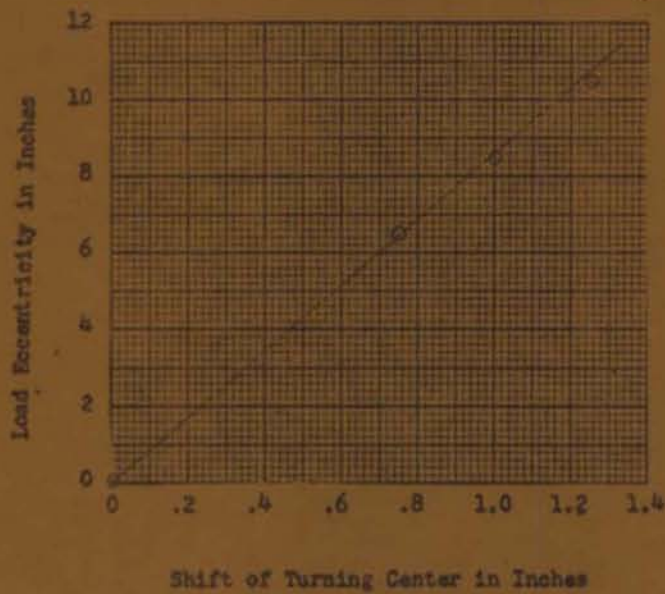


Figure 24

Computer Programs for Data Reduction and Design

```

PROGRAM STRESS          SIXTY
READ 75,NOP, EMU, E
DIMENSION EPA(200), EP3(200), EPC(200), TH(200), AM(200), EP1(200),
1 EP2(200), SIG1(200), SIG2(200), TAU(200)
READ 76,(EPA(I), EPB(I), EPC(I), I=1,NOP)
DO 10 I=1,NOP
AM(I)=(EPA(I)+ EPB(I)+ EPC(I))/3.
R=SQRT((EPA(I)-AM(I))*2+ ((EPC(I) -EPB(I))/1.73205)**2)
TH(I)=(ATANF((EPC(I) -EPB(I))/1.73205)/(EPA(I) -AM (I))))/2.)*5
17.2958
EP1(I)=AM(I)+R
EP2(I)=AM(I)-R
SIG1(I)=(E/(1.-EMU**2))*(EP1(I)+EMU*EP2(I))
SIG2(I)=(E/(1.-EMU**2))*(EP2(I)+EMU*EP1(I))
10 TAU(I)=(SIG1(I)-SIG2(I))/2.
PRINT 77,(I, EP1(I), EP2(I), SIG1(I), SIG2(I), TH(I), TAU(I), I=1,NOP)
STOP
75 FORMAT(13,2F20.8)
76 FORMAT(3F 20.9)
77 FORMAT(14,6E 15.8)

```

```

PROGRAM DESIGN
DIMENSION XRAY(14), FORCE(14), TAU(14,14), PHI(14,14)
READ 74, NX, NFO
74 FORMAT (2I2)
75 READ 75,(XRAY(I), FORCE(I), I=1,NFO)
75 FORMAT(2F10.0)
DO 11 I=1,NX
DO 12 J=1,NFO
RHO=SQRT((XRAY(I)**2)+6.25)
STRESS1=(FORCE(J)+10.50000*RHO)/20.62
STRESS2=FORCE(J)/2.48
STRESSH=(STRESS1+2.51/RHO)
STRESSV=(STRESS1-XRAY(I))/RHO
STRESSV=STRESSV+STRESS2
PHI(J,I) =ATANF(STRESSV/STRESSH)
12 TAU(J,I) =SQRT((STRESSH**2)+(STRESSV**2))
11 CONTINUE
PRINT 77
77 FORMAT(14X,5HFORCE,14X,4HXRAY,16X,3HTAU,14X,3HPHI)
DO 18 J=1,NFO
18 PRINT 76 (FORCE(J), XRAY(I), TAU(J,I), PHI(J,I), I=1,NX)
76 FORMAT(4X,4E20.8)
STOP
END
END

```